CIVIL ENGINEERING STUDIES
STRUCTURAL RESEARCH SERIES NO. 364

NUMERICAL METHODS FOR THE ANALYSIS OF BUCKLING AND POSTBUCKLING BEHAVIOR OF ARCH STRUCTURES

by
J. F. Harris
A. R. Robinson

A Technical Report
of a Research Program
Sponsored by
THE OFFICE OF NAVAL RESEARCH
DEPARTMENT OF THE NAVY
Contract No. N 0014-67-A-0305-0010
Project NAVY-A-0305-0010

UNIVERSITY OF ILLINOIS
URBANA, ILLINOIS
SEPTEMBER, 1970

NUMERICAL METHODS FOR THE ANALYSIS

of

BUCKLING AND POSTBUCKLING BEHAVIOR OF ARCH STRUCTURES

by

J. F. Harris

A. R. Robinson

A Technical Report

of a Research Program

Sponsored by

THE OFFICE OF NAVAL RESEARCH

DEPARTMENT OF THE NAVY

Contract No. N 0014-67-A-0305-0010

Project NAVY-A-0305-0010

UNIVERSITY OF ILLINOIS

Urbana, Illinois

September, 1970

ACKNOWLEDGEMENT

This report was prepared as a doctoral dissertation by Mr. John F. Harris and was submitted to the Graduate College of the University of Illinois at Urbana-Champaign in partial fulfillment of the requirements for the degree of Doctor of Philosophy in Civil Engineering. The work was done under the supervision of Dr. Arthur R. Robinson, Professor of Civil Engineering.

The investigation was conducted as part of a research program supported by the Office of Naval Research, Contract N00014-67-A-0305-0010, "Numerical and Approximate Methods of Stress Analysis". During the course of the investigation, Mr. Harris held a National Defense Education Act, Title IV, Fellowship.

The authors wish to thank Dr. Leonard Lopez, Assistant Professor of Civil Engineering, for his invaluable assistance in certain phases of the computer programming.

The numerical results were obtained with the use of the IBM 360-75 computer system of the Department of Computer Science of the University of Illinois at Urbana-Champaign.

TABLE OF CONTENTS

LIST OF TABLES

LIST OF FIGURES

1. INTRODUCTION

1.1. Object and Scope

The main objective of this study is to develop a set of numerical methods suitable for investigating the load-deflection and bifurcation characteristics of structures for which significant nonlinear behavior is possible. The methods are applicable to a wide variety of structures, but will be examined in detail only with reference to one of the simplest types of structures possessing the necessary complications in behavior - the planar arch under a concentrated load.

The term "planar", as used in this study, refers to the configuration of the arch during the initial stages of loading (often called the prebuckling configuration). Both in-plane and out-of-plane buckling behavior of the planar configuration are examined. Although it would be possible to include the effect of certain nonlinear stress-strain laws, the nonlinear behavior examined in this study is geometrical in nature and results from large displacements (arising from large rotations but small strains).

The numerical methods developed here are capable of determining limit points on the load-deflection curve (see Fig. 2, points A and B), as well as finding bifurcation points and subsequently tracing the buckled configuration. The numerical results given in Chapter 5 illustrate these capabilities in problems of considerable technical interest.

1.2. General Remarks and Observations

From the earliest work on the buckling of cylindrical shells, it has been noted that experimentally determined buckling loads of various

In view of this wide variety of possible behavior of structural members a consideration of postbuckling behavior is an essential part of the analysis of a given structure which exhibits a buckling phenomenon.

1.3. Background

As mentioned above, the numerical methods developed in the present study are applied to the simplest structures which exhibit the nonlinear behavior necessary to provide an adequate test of the methods. The mathematical model of the structures studied here is given by Love (1927) for the equilibrium forms of thin rods. According to Love, Clebsch (1862) and Kirchloff (1859) arrived independently at the equilibrium equations. The geometrical relationships are attributed to Routh (1905), and Clebsch (1862) is given credit for the moment-curvature relationships. These equations presented by Love are applicable to the three-dimensional behavior of thin, linearly elastic rods with inextensional centerlines, although an indication is given by Love of the necessary modification for an extensional centerline. Vlasov (1959) indicates, that as a first approximation, the effect of warping restraint on the behavior of curved beams may be introduced by using the corresponding relationship between torque and rate of twist for a straight rod. In Chapter 5, results are presented for the in-plane buckling of arches where the effect of extension of the centerline is included and for the lateral buckling of an I-beam where warping restraint is considered.

The oldest analysis of buckling, Euler's work on a perfect elastic column, (see Timoshenko and Gere (1961)) included a postbuckling analysis. However, the perfect column is one case in which the behavior

results for various rise-to-span ratios. The mathematical model assumed an inextensional centerline. It is not clear whether or not extension of the centerline would complicate this computational method, which involved elliptic integrals.

1.4. Outline of the Method of Analysis

In this study a set of numerical techniques is developed for improving an approximation to a bifurcation point on the load-deflection curve. One method permits a direct computation of an approximate eigenvector which is then improved simultaneously with the prebuckling configuration.

The technique requires a solution of a set of nonlinear equations which indicate how the prebuckling configuration (including the loading) must be modified in order to reach the bifurcation point. This part of the solution is treated in Chapter 2 in a mathematical fashion and in Chapter 4 for a specific physical problem. The nonlinear equations are developed with reference to the general eigenvalue problem $A X = \lambda B X$ and are solved by a modification of the Newton-Raphson method.

As indicated, the solution process predicts how the prebuckling configuration must be changed to reach a bifurcation point. The process of modifying the prebuckling configuration is examined in Chapter 3. The standard Newton-Raphson procedure may be used except when the prebuckling configuration is near a bifurcation point. As noted by Thurston (1969), the equations specifying the linear changes in the prebuckling configuration become singular at bifurcation points. A method proposed in this

study actually makes use of this fact to arrive at an improved prebuckling configuration and a better estimate of the eigenvector in a rapidly convergent computation.

1.5. Nomenclature

The symbols used in this study are defined in the text when they first appear. For convenient reference, the more important symbols are summarized here in alphabetical order. Some symbols are assigned more than one meaning; however, in the context of their use there are no ambiguities.

a	radius of undeformed circular arch
A, B, C	general linearlized operators, may be matrices differential or integral operators
b	constant vector
C, $\bar{C}$, D, $\tilde{D}$	coefficient matrices of linear algebraic equations
det(x)	determinant of x
d_i	deflection components at concentrated load, in global coordinates i = 1, 2, 3
e	scalar error term
EI_i	flexural rigidities (includes St.-Venant torsional rigidity), i = 1, 2, 3
E_I, δE_I	the I^{th} configuration and its corresponding increment in the Newton-Raphson procedure
EC_W	warping rigidity
H	rise of undeformed arch
I_1	for a planar member, moment inertia about an axis perpendicular to the plane
I_2	for a planar member, moment of inertia about an axis in the plane
I_3	corresponds to J, the St.-Venant torsion constant

2. PROCEDURE FOR FINDING BIFURCATIONS

2.1. General

A study of postbuckling behavior requires at least two items of information. These are the buckling load, along with the corresponding configuration just prior to buckling, and the eigenvector, which gives an initial estimate of the postbuckling path. In the following sections theoretical considerations are presented which lead to the development of a set of efficient numerical methods for treating bifurcations from a nonlinear prebuckling state. Detailed descriptions of the numerical procedures are reserved for Chapters 3 and 4.

2.2. Bifurcation as an Eigenvalue Problem

The eigenvalue problems to be treated here are assumed to be described by

$$A\,X = \lambda\,B\,X \tag{2.1}$$

and appropriate boundary conditions where necessary. The quantities A and B may be matrices, differential, or integral operators; λ is the eigenvalue and X the eigenvector. The operators A and B refer to the prebuckling configuration and are in general dependent on the eigenvalue λ but not on the eigenvector X. It is assumed that the dependence of A and B on λ is known, at least implicitly.

The discrete (algebraic) eigenvalue problem may be represented by Eq. (2.1) when A and B are interpreted as matrices. One technique that has been used to solve this type of problem is to increment the trial

α	non-dimensionalized buckling load (out-of-plane), $\alpha = Pa^2/\sqrt{EI_2GJ}$
β	non-dimensionalized buckling load (in-plane) $\beta = Pa^2/EI_1$
δ	increment operator
ε_{ijk}	alternating tensor
ε_c	strain of centerline
λ, $\bar{\lambda}$, λ_{cr}	eigenvalues
*	used to denote eigenvector quantities

eigenvalue λ (which in general implies changing A and B) and at each value of λ to compute the determinant of $(A - \lambda B)$. This procedure was used by Leicester (1968) and in essence is an extension of the so-called Holzer method, Holzer (1921). A change of sign of this determinant between successive values of the trial eigenvalue indicates an eigenvalue falling in that range. Interpolation may be used to find the value of λ for which det $(A - \lambda B)$ is zero. At this stage, the eigenvector may be generated in the conventional manner by setting one of the components of X to unity (say X_1) and solving for the other components on this basis. It may be appropriate to mention that det $(A - \lambda B)$ equal to zero does not necessarily imply bifurcation. It may mean that there is a limit point on λ, and some other quantity should be incremented.

The linearized equation governing the local behavior of the branch of the equilibrium curve corresponding to the prebuckling configuration is of the form $(A - \lambda B)\ Y = b$. It is then evident from Eq. (2.1) that an impending singularity of $(A - \lambda B)$ will cause numerical difficulties associated with changing the prebuckling configuration in the vicinity of a bifurcation point. That is, changes in A, B, and Y will not be accurate. This has been noted previously by Thurston (1969), who presented a computational device for the solution in that case. This same phenomenon has been encountered in this study and the means of compucation which has been devised is introduced in the next section. It will be seen to be less involved than that presented by Thurston.

The continuous eigenvalue problem may be solved in a manner similar to the discrete problem. In this case, however, it is not det $(A - \lambda B)$ which is examined but rather the determinant corresponding to

satisfaction of the boundary conditions. This technique has been used by Cohen (1965), Kalnins (1964) and Zarghamee and Robinson (1967). As with the discrete problem, there may be numerical difficulties in determining accurate changes in the prebuckling configuration near bifurcation points.

2.3. A New Solution Technique

An essential characteristic of the technique presented here is the simultaneous improvement of the bifurcation point (load and configuration) and the eigenvector by a process involving the interaction between the two.

If the A, B, and λ corresponding to a particular prebuckling configuration and an approximate eigenvector are substituted into Eq. (2.1), then

$$\{ A X - \lambda B X \}^{(j)} = R^{(j)} \tag{2.2}$$

where the superscript j indicates the j^{th} approximation and R is a residual. The object then is to remove the residual from Eq. (2.2). In the usual eigenvalue problem, λ is not treated as an unknown of the same type as X. However, the method proposed here considers λ B X as a nonlinear term. This suggests that some modification of the well-known Newton-Raphson procedure may be applicable here. Use of the standard Newton-Raphson technique has been discussed by Kalnins and Lestingi (1967), Leicester (1968) and West and Robinson (1969). In order to extend the Newton-Raphson technique to bifurcation problems, it is

necessary to linearize Eq. (2.1) about some known configuration (say the j^{th}). In essence, Eq. (2.1) is expanded about the j^{th} configuration and only the linear terms are kept.

The linearization of Eq. (2.1) yields

$$\{A\delta X - \lambda B\delta X\}^{(j)} = \{-\delta A X + \delta\lambda B X + \lambda\delta B X - R\}^{(j)} \tag{2.3}$$

Since A and B are in general dependent on λ, the linear parts of the increments of A and B may be formally expressed as

$$\delta A = \left.\frac{\partial A}{\partial \lambda}\right|_{\lambda=\lambda^{(j)}} \delta\lambda \quad , \quad \delta B = \left.\frac{\partial B}{\partial \lambda}\right|_{\lambda=\lambda^{(j)}} \delta\lambda \tag{2.4}$$

Substitution of Eqs. (2.4) into Eq. (2.3) results in

$$\{A\delta X - \lambda B\delta X\}^{(j)} = \{\delta\lambda(-\frac{\partial A}{\partial \lambda} X + BX + \lambda \frac{\partial B}{\partial \lambda} X) - R\}^{(j)} \tag{2.5}$$

Examination of Eq. (2.3) reveals there are two types of incremental quantities to be considered; those corresponding to changes in the eigenvector δX and those corresponding to changes in the prebuckling configuration $\delta\lambda$, δB, and δA. From Eq. (2.4), δA and δB are related to $\delta\lambda$ so that in fact, the unknowns are δX and $\delta\lambda$, as indicated in Eq. (2.5).

Once the quantities $\frac{\partial A}{\partial \lambda}$, $\frac{\partial B}{\partial \lambda}$ and an approximate eigenvector are computed, the solution of Eq. (2.5) may proceed as follows. Since $\delta\lambda$ is an unknown, there is one more unknown than there are equations to solve, a situation that does not arise in the usual Newton-Raphson technique. The presence of an extra unknown is to be expected, since the amplitude

of the eigenvector is indeterminate. The arbitrariness in the eigenvector is removed by specifying a scalar side condition

$$X^T B \, \delta X = 0 \tag{2.6}$$

This side condition (or its integral equivalent when appropriate) allows a solution for δX and $\delta\lambda$ by eliminating the possibility of large changes in the eigenvector if the eigenvalue and approximate eigenvector are nearly correct.

If the computed $\delta\lambda$ is not satisfactorily small, the prebuckling configuration is not one corresponding to an eigenvector and must be modified. The magnitude of $\delta\lambda$ dictates how the procedure continues. In essence, this method predicts approximately how λ and the prebuckling configuration should be changed to approach a bifurcation point.

For the above solution process, it has been implicitly assumed that the quantities $\frac{\partial A}{\partial \lambda}$, $\frac{\partial B}{\partial \lambda}$ could be computed. From Eq. (2.5) it appears that these quantities could be obtained by computing δA and δB for a unit value of $\delta\lambda$ ($\delta\lambda = 1$). This is a straightforward application of the Newton-Raphson procedure. However, as mentioned in Chapter 1, the equations become singular at bifurcation points. This means that at or near bifurcation points, a special computational device must be incorporated into the Newton-Raphson technique in order to compute changes in the prebuckling configuration accurately. This special computational device is discussed in the next section.

2.4. Numerical Treatment of the Singular Equations

As mentioned above, the direct procedure for changing the prebuckling configuration is bound to fail at or near the bifurcation point. The difficulty is caused by impending singularity of the operator $(A - \lambda B)$ as the bifurcation point is approached, and is manifested by ill-conditioned equations leading to unreliable values for the changes in the prebuckling configuration. A technique has been devised which actually uses the fact that the operator $(A - \lambda B)$ is singular to determine the changes in the prebuckling configuration accurately.

As Koiter (1945) points out, the eigenvector is orthogonal to changes in the prebuckling configuration at the bifurcation point. A side condition is thus available in the form

$$X^T C \quad Y = 0 \tag{2.7}$$

or in the form of an equivalent integral expression when X and Y are continuous quantities. The X and Y refer to the eigenvector and incremental change of the prebuckling configuration, respectively. The quantity C is a suitable self-adjoint positive-definite operator. This device is employed only for the determination of accurate changes in the prebuckling configuration near the bifurcation point. The actual choice of C is indicated for a particular example in Chapter 4.

The addition of Eq. (2.7) to the system of equations to be solved for the incremental changes in the prebuckling configuration means there are now more equations than unknowns. Actually the equations are not all

independent at the bifurcation point. It appears to be easiest, from a computational standpoint, to derive an independent set of equations by pre-multiplying the equations by the transpose of the coefficient matrix. This is equivalent to the so-called least-squares technique. Indeed, away from the bifurcation point, a least-squares interpretation of the computation is appropriate because the equations are independent. Appending the side condition to the original equations results in

$$D\,y = b \tag{2.8}$$

where D has one more row than column. The least squares solution of Eq. (2.8) yields

$$D^T D\,y = D^T b \tag{2.9}$$

For the algebraic eigenvalue problem, the matrix $D^T D$ may be shown to be nonsingular (see Appendix B).

2.5. The Initial Eigenvector

The method of generating the initial eigenvector is most easily explained in the context of a particular problem and solution technique. However, in Section 2.2 of this chapter, a method of generating the eigenvector for the algebraic eigenvalue problem is outlined for the special case of A, B and λ corresponding to the onset of buckling. An approximate eigenvector may be generated in the same way even though A, B and λ do not correspond to buckling. It has been found that some care must be taken in the process of finding the approximate eigenvector. This matter will be discussed in detail in Chapter 4.

2.6. Observations and Comments

Although the technique is examined for the cases when A and B depend on the eigenvalue λ, it should be evident that several types of less complicated eigenvalue problems are encompassed by this general theory. For instance, buckling loads of Euler struts and the modes of small-amplitude free vibration of elastic systems are examples where A and B do not depend on the eigenvalue. In fact, the technique was first tested on these simpler problems.

By restricting A and B to be self-adjoint and positive-definite, it is possible to place some aspects of the proposed method on a firm theoretical basis (see Appendices A and B). In addition, physical arguments and experience in solving a number of problems provide considerable evidence for the wide applicability of the method.

A paper by Rall (1961) proposed an iterative procedure for finding eigenvalues and eigenvectors of a discrete system. There is a formal relation between Rall's method and the present one, but in Rall's method the eigenvalue is not treated as an unknown the same basis as the components of the eigenvector. Further, in Rall's method there is no freedom in the choice of a "side condition" and, in fact, an unfortunate choice of co-ordinates can lead to failure of the procedure.

3. THE PREBUCKLING CONFIGURATION

3.1. Introduction

In Chapter 2, a general technique is presented for the simultaneous improvement of an approximate bifurcation point and eigenvector. There the technique is presented generally and, therefore, somewhat abstractly. In Chapters 3 and 4 the solution process for the buckling of a rod-type member is presented in some detail as an example of the use of the general technique of Chapter 2. The nature of the technique requires a method of determining an equilibrium configuration corresponding to a given load level which in general is given by the solution of a system of nonlinear equations. The procedure for solution of the nonlinear equations at some distance from a bifurcation point is presented in this chapter.

3.2. Problem Description

For a detailed analysis of the arch problem, the equations expressing the three-dimensional behavior of a rod-type member will be presented and their method of solution described. Since the boundary conditions and loading are pertinent to the analysis, a specific choice must be made. Here the member will be assumed to be clamped at the boundaries and loaded with a concentrated load (see Fig. 3(b) and Fig. 4).

As mentioned in Chapter 1, the equilibrium, geometric and moment-curvature relationships are those presented by Love (1927). Love also indicates how these equations must be modified in order to include the effects of extension of the member centerline In this study, extension of the centerline is neglected for the full three-dimensional problems, although results will be presented in Chapter 5 for some two-dimensional

problems where extension of the centerline is included. The effects of restraint of warping of the member cross section are not included in the discussion of this chapter, but results are presented in Chapter 5 for lateral buckling of an initially straight I-beam under a dead load where warping restraint is considered. Timoshenko and Gere (1961) and Vlasov (1959) indicate the formulation of the proper equations relating the twist of the member to the torsional moment when restraint of warping is considered.

3.3. Basic Equations for the Behavior of an Initially Curved Member

3.3.1. Preliminaries

Figure 1 shows the member and global coordinate system. Two of the member axes are taken as the principal axes of the section and the third is directed along the tangent to the centerline of the member. The member and global coordinate systems are related by the following matrix transformation.

$$\begin{Bmatrix} x_1 \\ x_2 \\ x_3 \end{Bmatrix} = \begin{bmatrix} \ell_1 & m_1 & n_1 \\ \ell_2 & m_2 & n_2 \\ \ell_3 & m_3 & n_3 \end{bmatrix} \begin{Bmatrix} X_1 \\ X_2 \\ X_3 \end{Bmatrix} \tag{3.1}$$

where the ℓ_i, m_i, and n_i's are direction cosines.

3.3.2. Equilibrium Equations

The equations of equilibrium, as presented by Love (1927) may be written as

$$\frac{dN_i}{ds} - \varepsilon_{ijk} K_j N_k = 0$$

$$\frac{dM_i}{ds} - \varepsilon_{ijk} K_j M_k - \varepsilon_{3ik} N_k = 0 \qquad (3.2)$$

The summation convention will be used throughout, unless the contrary is specifically stated. Also, the subscripts i, j, k will always take on the values 1, 2, 3. The quantities N_i, M_i, K_i are internal forces, internal moments and curvature vectors, respectively, in the local coordinate system. The quantity ε_{ijk} is the alternating tensor and s is the arc length.

3.3.3. Geometric Equations

Although there are only three independent direction cosines, it is convenient to ignore this fact temporarily and to present the entire set of geometric equations. The nine equations, relating direction cosines to curvatures are

$$\frac{d\ell_i}{ds} - \varepsilon_{ijk} \ell_j K_k = 0$$

$$\frac{dm_i}{ds} - \varepsilon_{ijk} m_j K_k = 0 \qquad (3.3)$$

$$\frac{dn_i}{ds} - \varepsilon_{ijk} n_j K_k = 0$$

3.3.4. Displacement Equations

The equilibrium and geometric equations do not involve displacements explicitly. However, the equations expressing satisfaction of the boundary conditions do, in general, involve displacements. The displacement quantities required are derivable from the direction cosines by a simple quadrature.

$$X_1(s) = \int_0^s l_3(\xi)\, d\xi$$

$$X_2(s) = \int_0^s m_3(\xi)\, d\xi \qquad (3.4)$$

$$X_3(s) = \int_0^s n_3(\xi)\, d\xi$$

where ξ is a dummy variable and the $X_i(s)$ are the global coordinates of the centerline of the member as functions of the arc length, s.

3.3.5. Moment-Curvature Relations

The effects of restraint of warping are not considered in the behavior of the arches studied here. Thus the torsional behavior is entirely of the St.-Venant type. The torque is given by the product of the change of the rate of twist, $K_3 - K_{30}$, and the St.-Venant torsional rigidity, GJ. For consistency of notation, GJ is taken equal to EI_3.

Thus the moment-curvature relations become

$$M_i = EI_i \, (K_i - K_{i0}), \text{ (no summation, } i = 1, 2, 3) \tag{3.5}$$

where EI_i refers to the various rigidities and K_{i0} is the curvature vector in the unloaded state.

3.3.6. Conditions at a Concentrated Load

The global representation of the concentrated load is taken as

$$\overline{P} = P \, \overline{I}_2 \tag{3.6}$$

where $\overline{I}_2$ is a unit vector in the global X_2 direction and P is the magnitude of the force, which is assumed to be applied at the centerline of the member.

Consideration of equilibrium of an element of arch containing the concentrated force yields the following "jump conditions" relating the internal force resultants on either side of the load.

$$N_i^{(+)} + P \, m_i - N_i^{(-)} = 0 \tag{3.7}$$

The superscripts +, -, refer to points to the right and left of the load, positive being in the direction of increasing arc length.

3.3.7. Boundary Conditions for a Clamped Arch

For a clamped arch, the boundary conditions specify that both the direction cosines at the supports and the global coordinates of the

supports remain unchanged. The boundary conditions for an initially planar clamped arch are

$$\begin{aligned} \ell_2 &= \ell_{20} \\ m_1 &= m_{10} \qquad (\text{at } s = 0,\ s = s_f) \\ n_3 &= n_{30} \\ X_i &= X_{i0} \end{aligned} \tag{3.8}$$

where the second subscript 0 indicates the original configuration and s_f is the arc coordinate of the far boundary.

3.3.8. Complementary Loading Parameter

It has been noted previously by Bueckner, Johnson and Moore (1965) and Leicester (1968) that a numerical analysis of snap-through buckling of shallow spherical shells can encounter difficulties associated with the incremental loading process. A similar difficulty occurs in arches. This difficulty stems from the fact that so-called limit points (see Fig. 2) may exist on the force-deflection curve. If, near point A an increment of force is chosen such that the total force is greater than P_A, obviously there is no solution. This is a very real possibility since in general the maximum value P_A is not known in advance. Near point A, the difficulty may be overcome by incrementing the deflection instead of the force. A similar situation occurs near point B except that the force quantity should be incremented instead of the deflection. In the vicinity of the limit points, convergence of the Newton-Raphson or successive approximation procedures will be slow or fail entirely if a poor choice of loading parameter is made. For this

reason it is advantageous to be able to select either force or deflection as the independent variable in the loading process.

In order to demonstrate how a loading parameter other than the concentrated force itself is used in the solution process, a complementary loading parameter corresponding to the deflection under the concentrated force and in the direction of the force will be used here. The expression for this component of the deflection under the load is

$$d_2 = \int_0^{s_p} \{m_3(\xi) - m_{30}(\xi)\}\, d\xi \tag{3.9}$$

where the upper limit of integration, s_p, refers to the arc-length coordinate of the point of application of the force.

3.4. Solution of Nonlinear Equations

3.4.1. General Discussion

There are several techniques available for solving two-point boundary value problems described by nonlinear ordinary differential equations. The character of the particular set of equations may limit the effectiveness of some of these techniques.

One particular technique called the "shooting method" has been used by Huddleston (1968) to solve the nonlinear equations which describe the large deflections of an arch under a concentrated load. The boundary value problem is converted to an initial value problem and the nonlinear

equations integrated numerically. Since some of the initial values are unknown, these are adjusted until the far boundary conditions are satisfied. Generally a few iterations are required to satisfy the boundary conditions. This technique will encounter numerical difficulties when the solution of the nonlinear ordinary differential equation can exhibit a boundary layer or edge effect. In this case, the initial value solutions will grow rapidly as they are propagated to the far boundary. Since computers carry a finite number of digits in numerical computations, the quantities required for the equations which express satisfaction of the far boundary conditions may have literally no significance because of round-off during the numerical integration process. In fact, this phenomenon can occur even though the initial values are quite close to the correct ones.

Another technique has been developed by Berezin and Zhidkov (1960) and by Jordan and Shelley (1966) for solving just the type of problem where "growing" solutions are present. This technique does not require iteration but a transformation of the equations to a new set of variables is necessary before the solution may proceed. As with the "shooting method", the transformed set of equations is integrated numerically since they are in general nonlinear. Jordan and Shelley indicate that if the original problem does not have a boundary or edge effect, the transformed solution may. In this case, the transformed problem would encounter numerical difficulties. It turns out that even if there is a boundary effect, it is possible that the method will fail.*

The technique used in this study does not depend on the character of the nonlinear equations. That is, the presence of a boundary or edge

---

* This observation is due to Professor M. S. Zarghamee.

effect does not present any serious obstacles. The Newton-Raphson technique is used to solve the nonlinear equations and thus only linearized equations are integrated. When growing solutions are present in the integration of the linearized equations, the suppression technique used by Zarghamee and Robinson (1967) and Goldberg, Setlur and Alspaugh (1965) is implemented to avoid the loss of significant figures due to round-off.

3.4.2. The Newton-Raphson Procedure

The nonlinear equations of this study are solved using the Newton-Raphson procedure. In the use of this procedure, the loading is applied to the structure in increments (not necessarily small) by the following computational process. The reason for applying the loading parameter in steps will become apparent as the discussion proceeds.

Assume that at some stage in the loading process a solution E_I of the nonlinear equations is known which corresponds to a loading level L_I. An increment of load ΔL_I is now applied. The Newton-Raphson procedure is used to find a new equilibrium configuration corresponding to the total loading parameter given by $L_I + \Delta L_I$. The equations specifying the linear response of the configuration E_I must then be derived by linearizing the equations about this configuration. The linear incremental solution δE_I corresponding to an increment of loading ΔL_I is added to the existing configuration E_I to produce a new configuration E_{I+1}. In general the configuration E_{I+1} will not satisfy the nonlinear equations since a linear approximation was used to compute δE_i. Thus there are residuals in these nonlinear equations.

The next step is to remove the residuals, without a further increase in the loading parameter. The equations are again linearized, this time about the new configuration E_{I+1}. The linear response o E_{I+1} at this configuration is calculated. The "loading" in this computation consists of the negatives of the residuals in the corresponding nonlinear equations. A new configuration E_{I+2} equal to $E_{I+1} + \delta E_{I+1}$ is thus derived. At this point, the configuration E_{I+2} is substituted into the nonlinear equations and the resulting residuals are again examined. If the residuals are small enough, a new equilibrium configuration has been found and another increment of the loading parameter may be applied. If the residuals are not satisfactory, this process of removing residuals, for a constant value of loading parameter, is repeated until a new equilibrium configuration is obtained.

It is evident from the above discussion that it is necessary to linearize the nonlinear equations of Sections 3.3.2. - 3.3.8. about a general reference configuration in order to use the Newton-Raphson procedure. These linearized equations are presented in the next section.

3.4.3. Linearization of the Prebuckling Configuration

In order to avoid the cumbersome notation of Chapter 2 in expressing the linearized equations of the arch problem, the superscript j used in Chapter 2 to denote the j^{th} configuration will be dropped and instead the current configuration will instead be denoted simply by the quantities, N_i, M_i, K_i, ℓ_i, m_i, n_i, etc. without a superscript. Since the equations specifying the prebuckling configuration are of first-order, the linearization process is particularly straightforward and leads to the following equations.

Linearized Equilibrium Equations:

$$\frac{\delta(dN_i)}{ds} - \varepsilon_{ijk}\,(\delta K_j\, N_k + K_j\, \delta N_k) = 0$$

$$\frac{\delta(dM_i)}{ds} - \varepsilon_{ijk}\,(\delta K_j\, M_k + K_j\, \delta M_k) - \varepsilon_{3ik}\,\delta N_k = 0 \qquad (3.10)$$

Linearized Geometric Equations:

$$\frac{\delta(d\ell_i)}{ds} - \varepsilon_{ijk}\,(\delta K_j \ell_k + K_j\, \delta \ell_k) = 0$$

$$\frac{\delta(dm_i)}{ds} - \varepsilon_{ijk}\,(\delta K_j\, m_k + K_j\, \delta m_k) = 0 \qquad (3.11)$$

$$\frac{\delta(dn_i)}{ds} - \varepsilon_{ijk}\,(\delta K_j\, n_k + K_j\, \delta n_k) = 0$$

Linearized Displacement Equations:

$$\delta X_1 = \int_0^s \delta \ell_3\,(\xi)\; d\xi$$

$$\delta X_2 = \int_0^s \delta m_3\,(\xi)\; d\xi \qquad (3.12)$$

$$\delta X_3 = \int_0^s \delta n_3 (\xi)\, d\xi \tag{3.12}$$

Linearized Moment-Curvature Relations:

$$\delta M_i = (EI)_i \, \delta K_i \quad , \text{ (no summation)} \tag{3.13}$$

Linearized Condition at the Concentrated Load:

$$\delta N_i^{(+)} - \delta N_i^{(-)} + P \, \delta m_i + \delta P \, m_i = 0 \tag{3.14}$$

Linearized Boundary Conditions:

$$\left.\begin{aligned} \delta \ell_2 &= 0 \\ \delta m_1 &= 0 \\ \delta n_3 &= 0 \\ \delta X_i &= 0 \end{aligned}\right\} \quad (\text{at } s = 0,\ s = s_f) \tag{3.15}$$

Linearized Complementary Loading Parameter:

$$\Delta d_2 = \int_0^{s_p} \delta n_3 (\xi)\, d\xi \tag{3.16}$$

The δN_i, δM_i, δK_i, $\delta \ell_i$, δm_i, δn_i, δd_2, etc., are the linearized quantities where the δ is used to denote a linear increment. In general,

Eqs. (3.10), (3.11), (3.12), (3.14), (3.15), (3.16) when they are applied, will have on their right hand sides not zeros but the negatives of the residuals computed from their corresponding nonlinear equations as explained in Section 3.4.2.

3.5. Typical Incremental Loading Cycle

The typical incremental loading cycle of this study may be summaried as follows using the notation which has been introduced:

(1) Assume that an equilibrium configuration corresponding to the quantities M_i, N_i, K_i, ℓ_i, m_i, n_i, d_2, etc. is known;

(2) Apply an increment Δd_2 of the loading parameter by use of the linearized equations (Eqs. (3.10) - (3.16)) to obtain δN_i, δM_i, δK_i, $\delta \ell_i$, δm_i, δn_i, Δd_2, etc.;

(3) Add the incremental quantities δN_i, δM_i, δK_i, $\delta \ell_i$, δm_i, δn_i, Δd_2, etc. determined in the previous step to the previous values of N_i, K_i, ℓ_i, m_i, n_i, d_2, etc. to obtain a new set of N_i, M_i, K_i, ℓ_i, m_i, n_i, d_2, etc.;

(4) Compute the residuals in Eqs. (3.2) - (3.9) using the new N_i, M_i, ℓ_i, m_i, n_i, d_2, etc. of step (3);

(5) Check the residuals to see if they are acceptable. If so, the process stops, a new equilibrium configuration having been determined. If the residuals are not acceptable, go on to step (6). Note there are, in general, residuals in the jump condition Eq. (3.7) and in the complementary loading parameter expression

Eq. (3.9) as well as the differential equations;

(6) Remove the residuals obtained in step (4) by computing the linear effect on the new configuration (determined in step (3)) of the negatives of the residuals determined in step (4). Go back to step (3).

Although the same equations are used in steps (2) and (6), (except for the right hand sides) the increase in the loading parameter d_2 is carried out only once. Note that the N_i, M_i, K_i, ℓ_i, m_i, n_i, d_2, etc. are always the latest quantities.

3.6. Details of the Solution of the Linearized Differential Equations

The discussion of a typical incremental loading cycle, Section 3.5, was based on the assumption that a solution to the two-point boundary value problem given by the linearized differential equations, boundary conditions, jump condition and incremental loading parameter, could be found. In this study, the modified two-point boundary value problem defined by the linearized differential equations, the boundary conditions, jump condition and the incremental loading equation is converted to an initial value problem. The initial value technique has been used by Kalnins (1964), Goldberg, Setlur, and Alspaugh (1965), and Zarghamee and Robinson (1967) to solve boundary value problems described by ordinary differential equations. Since the method uses one boundary as the origin of the linearized initial value problem, the so-called initial values are selected so as to satisfy the boundary conditions at the origin automatically. As the method is used here,

a set of independent initial value solutions (see Table 1) is propagated from the origin to the far boundary where a linear combination of these solutions is formed to satisfy the linearized boundary conditions and the condition on the incremental loading parameter Eq. (3.16).

The increments in the boundary displacements at the far end and in the loading parameter are expressed as integrals of the quantities occurring in the linearized differential equations. This means that the equations (incremental boundary conditions and incremental loading parameter) for determining the proper linear combination of solutions require that a quadrature of the quantities in the individual initial value solutions be carried out. This has been done numerically using Simpson's rule. The condition on the incremental loading parameter is treated the same as an additional boundary condition when forming the linear combinations necessary to solve for the correct initial values.

The individual initial value solutions are found by numerical integration using a trapezoidal integration formula as part of a predictor-corrector process. The numerical integration process has been presented by Crandall (1956). The character of these equations is such that rapidly growing solutions are not present in the numerical integration process. For this reason, the so-called suppression technique (see Section 3.4.1.) is not necessary. In Chapter 5 of this study, an example problem of the lateral buckling of an I-beam with warping rigidity is solved which requires suppression during the integration process.

Table 1 shows the initial values for each solution. The residual terms in the particular solution occur in what has been called step 4 of the incremental loading procedure as given in Section 3.5.

3.7. Direction Cosine Correction

Since the direction cosines are treated as independent quantities during the numerical integration of the linearized differential equations, it is possible that "drift" of the direction cosines will take place so that they will no longer form an orthonormal set. The computational process guarantees that the squares and scalar products of the new local coordinate basis vectors are constant across the arch. However there is no mechanism in the straightforward procedure to control drift in these constants, which should, of course, be either one or zero. A technique, outlined in Appendix C, has been developed to ensure orthonormality.

3.8. Other Boundary Conditions

An arch which is simply supported in the plane presents no added complications. The geometric boundary condition, $n_3 = n_{30}$ is replaced by the moment condition $M_1 = 0$. See Figs. 3(a) and 3(b).

Other types of boundary conditions may require considerable care in their formulation. If it is desirable to allow more than one free rotation at a support, it is useful to have in mind a physical model (say a Hooke's joint) of the support in order to avoid the possibility of introducing a nonconservative force system at the support. This difficulty has been explained in detail by Ziegler (1956).

4. DETERMINATION OF POINTS OF BIFURCATION IN THE CASE OF NONLINEAR PREBUCKLING BEHAVIOR

4.1. Introduction

As mentioned in Chapter 2, a study of postbuckling behavior requires the location of the bifurcation point. This chapter deals with a specific application of the general technique of Chapter 2 for improving an approximation to a bifurcation point and the corresponding approximate eigenvector. For the specific arch problem, a prebuckling configuration determined by the method of Chapter 3 is used as an approximation to the bifurcation point in the process described in Chapter 2. The method for generating the corresponding approximate eigenvector will be given in detail later in this chapter. Since this technique requires not only a knowledge of the local behavior of the prebuckling configuration (the Y of Sec. 2.2.) but also the eigenvector "branching" from a prebuckling curve (the X of Sec. 2.2.), two different incremental quantities must be studied at the same time. It is not difficult to adapt the linearized equations of Chapter 3 for this purpose with a suitable change of notation. The new linearized equations will be solved for the quantities corresponding to the eigenvector, which is "along" the initial segment of a new branch. These linearized equations will be referred to as "branch equations".

4.2. Branch Equations

The following equations are the linearized equations of Chapter 3 with the δ replaced by an asterisk. As the discussion proceeds, it will be

obvious that a new notation is necessary for clarity. These equations play the role of Eq. (2.1) of Chapter 2.

Branch Equilibrium Equations:

$$\frac{dN_i^*}{ds} - \varepsilon_{ijk}\,(K_j^*\,N_k + K_j\,N_k^*) = 0$$

$$\frac{dM_i^*}{ds} - \varepsilon_{ijk}\,(K_j^*\,M_k + K_j\,M_k^*) - \varepsilon_{3ik}\,N_k^* = 0 \qquad (4.1)$$

Branch Geometric Equations:

$$\frac{d\ell_i^*}{ds} - \varepsilon_{ijk}\,(K_j^*\,\ell_k + K_j\,\ell_k^*) = 0$$

$$\frac{dm_i^*}{ds} - \varepsilon_{ijk}\,(K_j^*\,m_k + K_j\,m_k^*) = 0 \qquad (4.2)$$

$$\frac{dn_i^*}{ds} - \varepsilon_{ijk}\,(K_j^*\,n_k + K_j\,n_k^*) = 0$$

Branch Displacement Equations:

$$X_1^*(s) = \int_0^s \ell_3^*(\xi)\,d\xi$$

$$X_2^*(s) = \int_0^s m_3^*(\xi)\,d\xi \qquad (4.3)$$

$$X_3^*(s) = \int_0^s n_3^*(\xi)\, d\xi \tag{4.3}$$

Branch Moment-Curvature Relations:

$$M_1^* = (EI)_i K_i^*, \quad \text{(no summation)} \tag{4.4}$$

Branch Condition at the Concentrated Load:

$$N_i^{*(+)} - N_i^{*(-)} + P m_i^* = 0 \tag{4.5}$$

Branch Boundary Conditions:

$$\begin{aligned} \ell_2^* &= 0 \\ m_1^* &= 0 \\ &\qquad (\text{at } s = 0,\ s = s_f) \\ n_3^* &= 0 \\ X_i^* &= 0 \end{aligned} \tag{4.6}$$

If the prebuckling configuration given by the quantities N_i, M_i, K_i, ℓ_i, m_i, n_i, etc. is the one corresponding to bifurcation, the eigenvector may be generated from Equations 4.1 - 4.6 in a straightforward manner. In general this fortuitous circumstance will not prevail and the prebuckling configuration must be adjusted in order to reach the bifurcation point. The crux of the problem then is to adjust the prebuckling configuration so that a better approximation to the bifurcation point is obtained. The general technique developed in Chapter 2 is used for this purpose.

Assume that an approximate prebuckling configuration found by the method of Chapter 3 and an approximate eigenvector are substituted into Eqs. (4.1) - (4.6). There is, in general, a residual in these equations. The modification of the Newton-Raphson technique introduced in Chapter 2 is used to remove the residuals. Here it is necessary to linearize the so-called branch equations with respect to the prebuckling (unstarred) quantities (N_i, M_i, K_i, ℓ_i, m_i, n_i, etc.) and the current approximate eigenvector (N_i^*, M_i^*, K_i^*, ℓ_i^*, m_i^*, n_i^*, etc.).

4.3. Linearized Branch Equations

As noted in Chapter 2, two types of incremental quantities appear in the linearized branch equations; those corresponding to changes of the prebuckling configuration (δN_i, δM_i, δK_i, $\delta \ell_i$, δm_i, δn_i, etc.) and those corresponding to changes in the eigenvector (δN_i^*, δM_i^*, δK_i^*, $\delta \ell_i^*$, δm_i^*, δn_i^*, etc.). The linearized branch equations are understood to be valid about a "hyper-configuration" consisting of the current prebuckling configuration and the approximate eigenvector. Also, in general, Eqs. 4.7, 4.8, 4.9, 4.11, and 4.12 will have non-zero right hand sides equal to the residuals computed from the corresponding nonlinear branch equation. The linearized branch equations, as given below, play the role of Eq. (2.3).

Linearized Branch Equilibrium Equations:

$$\frac{\delta dN_i^*}{ds} - \varepsilon_{ijk} (\delta K_j^* N_k + K_j^* \delta N_k + \delta K_j N_k^* + K_j \delta N_k^*) = 0 \quad (4.7)$$

Assume that an approximate prebuckling configuration found by the method of Chapter 3 and an approximate eigenvector are substituted into Eqs. (4.1) - (4.6). There is, in general, a residual in these equations. The modification of the Newton-Raphson technique introduced in Chapter 2 is used to remove the residuals. Here it is necessary to linearize the so-called branch equations with respect to the prebuckling (unstarred) quantities (N_i, M_i, K_i, ℓ_i, m_i, n_i, etc.) and the current approximate eigenvector (N_i^*, M_i^*, K_i^*, ℓ_i^*, m_i^*, n_i^*, etc.).

4.3. Linearized Branch Equations

As noted in Chapter 2, two types of incremental quantities appear in the linearized branch equations; those corresponding to changes of the prebuckling configuration (δN_i, δM_i, δK_i, $\delta \ell_i$, δm_i, δn_i, etc.) and those corresponding to changes in the eigenvector (δN_i^*, δM_i^*, δK_i^*, $\delta \ell_i^*$, δm_i^*, δn_i^*, etc.). The linearized branch equations are understood to be valid about a "hyper-configuration" consisting of the current prebuckling configuration and the approximate eigenvector. Also, in general, Eqs. 4.7, 4.8, 4.9, 4.11, and 4.12 will have non-zero right hand sides equal to the residuals computed from the corresponding nonlinear branch equation. The linearized branch equations, as given below, play the role of Eq. (2.3).

Linearized Branch Equilibrium Equations:

$$\frac{\delta dN_i^*}{ds} - \epsilon_{ijk} (\delta K_j^* N_k + K_j^* \delta N_k + \delta K_j N_k^* + K_j \delta N_k^*) = 0 \quad (4.7)$$

$$\frac{\delta dM_i^*}{ds} - \varepsilon_{ijk} (\delta K_j^* M_k + K_j^* \delta M_k + \delta K_j M_k^* + K_j \delta M_k^*)$$

$$- \varepsilon_{3ik} \delta N_k^* = 0 \qquad (4.7)$$

Linearized Branch Geometric Equations:

$$\frac{\delta d\ell_i^*}{ds} - \varepsilon_{ijk} (\delta K_j^* \ell_k + K_j^* \delta \ell_k + \delta K_j \ell_k^* + K_j \delta \ell_k^*) = 0$$

$$\frac{\delta dm_i^*}{ds} - \varepsilon_{ijk} (\delta K_j^* m_k + K_j^* \delta m_k + \delta K_j m_k^* + K_j \delta m_k^*) = 0 \qquad (4.8)$$

$$\frac{\delta dn_i^*}{ds} - \varepsilon_{ijk} (\delta K_j^* n_k + K_j^* \delta n_k + \delta K_j n_k^* + K_j \delta n_k^*) = 0$$

Linearized Branch Displacement Equations:

$$\delta X_1^*(s) = \int_0^s \delta \ell_3^* (\xi) \, d\xi$$

$$\delta X_2^*(s) = \int_0^s \delta m_3^* (\xi) \, d\xi \qquad (4.9)$$

$$\delta X_3^*(s) = \int_0^s \delta n_3^* (\xi) \, d\xi$$

Linearized Branch Moment-Curvature Relations:

$$M_i^* = (EI)_i \, K_i^* \quad , \quad \text{(no summation)} \tag{4.10}$$

Linearized Branch Condition at the Concentrated Load:

$$\delta N_i^{*(+)} - \delta N_i^{*(-)} + P\delta m_i^* + \delta P m_i^* = 0 \tag{4.11}$$

Linearized Branch Boundary Conditions:

$$\begin{aligned} \delta \ell_2^* &= 0 \\ \delta m_1^* &= 0 \\ & \qquad (\text{at } s = 0, \; s = s_f) \\ \delta r_2^* &= 0 \\ \delta X_i^* &= 0 \end{aligned} \tag{4.12}$$

Since the linearized branch equations contain incremental terms associated with changes of the prebuckling configuration (the unstarred quantities) a preliminary computation is necessary before the actual solution can proceed. This computation involves the determination of the linearized response of the prebuckling configuration for $\delta P = 1$; i.e., the counterpart here of the computation in Section 2.4. The method for carrying out this part of the solution of the linearized branch equations depends on how "close" the current prebuckling configuration is to the bifurcation point. Section 4.5 is devoted to this topic.

It is also necessary to compute an initial approximation to the eigenvector before solving the linearized branch equations, as it is the interaction of the approximate eigenvector with the prebuckling configuration that produces the residuals which "drive" the linearized branch equations. The computation of the approximate eigenvector is discussed in Section 4.6.

If the approximate prebuckling configuration is far enough from the bifurcation point to permit use of the standard Newton-Raphson technique for the purpose of obtaining changes in the prebuckling configuration, then the process of improving the eigenvalue and eigenvector is straightforward. The linearized branch equations would form a two-point boundary value problem except for the fact that δP is unknown also. The increments of the unstarred quantities and δP are the only unknowns. The extra unknown δP is to be expected since the amplitude of the eigenvector is indeterminate. In order to solve the system of linearized branch equations, a scalar side condition is appended to these equations. This side condition is taken as

$$\int_0^{s_f} M_i^* \, \delta K_i^* \, ds = 0 \tag{4.13}$$

This expression ensures that there are not large changes "parallel" to the eigenvector when the eigenvector is close to its true "direction".

The solution of these linearlized branch equations (with Eq. (4.13)) is quite similar to the solution of the linearized equations of Chapter 3.

The scalar side condition introduced here, Eq. (4.13), plays the role of the complementary loading parameter of Chapter 3. The modified boundary value problem described by Eqs. (4.7) - (4.12) and (4.13), is converted to an initial value problem. As in Chapter 3, a set of initial value problems is propagated from the origin to the far boundary where a linear combination of these solutions is formed to satisfy the boundary conditions and the scalar side condition. The procedure is similar enough to that of Chapter 3 that, in fact, the same numerical integration routine can be used in both parts of a computer program to solve the problem. The sets of initial values given in Table 1 carry over to the solution process here with the understanding that the incremental branch quantities are now the unknowns. An essential feature in the solution of the linearized branch equations is the presence of the incremental terms corresponding to changes of the prebuckling configuration. These terms appear only in the initial value solution corresponding to $\delta P = 1$ (see Table 1). This should be apparent since the prebuckling configuration can change only when P changes.

Once the value of δP is computed, the correct linearized change in the prebuckling configuration is easily found by scaling the changes caused by $\delta P = 1$, which are found in Section 4.5.

Thus, both the prebuckling configuration and the eigenvector are modified simultaneously.

4.5. Modifying the Prebuckling Configuration in the Vicinity of a Bifurcation Point

As indicated in Chapters 2 and 3, there are computational difficulties associated with computing the linearized response of the prebuckling

configuration accurately in the vicinity of bifurcation points. This section is devoted to a discussion of the solution to this problem.

The changes in the prebuckling configuration are required to be orthogonal to the eigenvector (see Section 2.4). For an inextensional centerline, this orthogonality relation is conveniently expressed as

$$\int_0^{s_f} M_i^* \, \delta K_i \, ds = 0 \tag{4.14}$$

The M_i^* used in Eq. (4.14) are the latest values obtained during the process of improving the bifurcation point and eigenvector. This extra condition is then appended to the initial value problem described in Chapter 3. There are now more equations than unknowns, but as mentioned in Chapter 2, all of these equations are valid at the bifurcation point. A consistent set of equations is derived using the least-squares technique.

This technique permits the accurate computation of changes in the prebuckling configuration near the bifurcation point. Note, however, that this device is essential only in the vicinity of the bifurcation point. At other points, the standard Newton-Raphson technique outlined in Chapter 3 is satisfactory for modifying the prebuckling configuration.

4.6. Generating the Approximate Eigenvector

The process of improving an eigenvalue involves the solution of a system of non-singular linear algebraic equations. The only difficulty is in arriving at a suitably "close" initial P and eigenvector. Since the

P used is only approximate, there will in general not exist a solution of the branch equations satisfying all the boundary conditions. The computational device which has been adapted here is to release one of the boundary conditions. In the first subsequent improvement of the P and eigenvector, it is a straightforward matter to reimpose the constraint which has been released.

It is obvious that there will, in general, be more than one choice of constraint which can be released for calculation of the initial approximation of the eigenvector. It has been found that by an unfortunate choice of release of constraint, it is possible to "skip" the eigenvalue being sought and "jump" to a distant one. The technique used to avoid this problem is to relax what appears to be the "softest" of the constraints. For instance, in out-of-plane buckling of an arch, the restraint corresponding to rotation about the tangent to the centerline at one end of the member is relaxed.

In general, it might be necessary to run through all choices of constraint release at one end to find the one leading to the smallest δP on the first cycle of improvement. However, this extra computation is actually not extensive.

4.7. Summary of the Typical Computational Cycle

The first part of the cycle is really a preparatory stage. The change in the prebuckling configuration for $\delta P = 1$ is computed and the approximate eigenvector is generated. Computational details are explained in Sections 4.5 and 4.6. At this point, the current prebuckling configuration

and the approximate eigenvector are substituted into the branch equations and residuals are computed. These residuals are used to "drive" the linearized branch equations.

Because of the way the approximate eigenvector is generated, during the first iteration step the residuals do not appear in the differential equations but only in the boundary condition which was violated when the approximate eigenvector was generated. For subsequent iterations, there are, in general, residuals in both the differertial equations and the boundary conditions.

Eventually, as successive prebuckling configurations are predicted and examined for the presence of an eigenvector, the value of δP and the residuals in the branch equations computed during this sequence will become acceptably small. At this point, the bifurcation load has been reached and the corresponding eigenvector generated.

The special process for obtaining changes in the prebuckling configuration when the standard Newton-Raphson technique fails because of poorly conditioned equations was never needed until the latest relative change in P was less than 0.10.

4.8. Postbuckling Paths

Without referring to the question of stability of the paths, it is a simple matter now to proceed onto the branch given initially by the eigenvector. This is done by adding a multiple of the eigenvector to the prebuckling configuration and then determining a new nonlinear configuration using the technique of Chapter 3.

Koiter (1945) indicates that if there is a single branch from the fundamental or prebuckling path, stability of the new path is determined by whether the load capacity increases or decreases. If the load increases, the new path is stable and if the load decreases, the new path is unstable.

If there is a multiple eigenvalue and multiple branches from the fundamental branch, the stability considerations are more complicated. Koiter (1945) has a discussion of this more difficult problem. In Appendix A of this study, a solution of the computational problem of determining multiple branches is indicated.

5. NUMERICAL RESULTS OF THE APPLICATION OF THE THEORY TO ARCHES AND BEAMS

5.1. General Remarks

In this chapter, several sample problems of the buckling of arches are presented. In addition, a few results are presented for lateral buckling of a beam. These problems are solved using the technique introduced in Chapters 2, 3, and 4. The chief object of these examples is to demonstrate some of the possibilities of the technique. Comparisons with previous work are made where such work is available.

The examples given in Sections 5.3.2. and 5.3.3. are planar arches which may buckle only in the plane of the arch (see Fig. (5(b)). Two sets of boundary conditions and two sets of rise-to-span ratios are considered. In Section 5.3.4., three-dimensional buckling of initially planar arches is considered. That is, the arches may deform in the plane and buckle out-of-plane. Two sets of boundary conditions and rise-to-span ratios are considered. In addition, results are also presented for an arch which first buckles in its plane, sways to the side, and subsequently buckles out-of-plane. In Section 5.3.5., lateral buckling of a beam with warping restraint is considered and two examples are presented.

5.2. Description of Problems

All the arches in problems involving three-dimensional behavior are assumed to have inextensional centerlines and to be fixed at the boundaries insofar as out-of-plane motion is concerned. In certain of the three-dimensional problems selected, rotations are permitted at the supports

about an axis perpendicular to the original plane of the arch (see Fig. 3(a)). The two-dimensional problems may involve either extensional or inextensional centerlines and, in addition, the arches may be fixed or simply-supported at the ends. The cross sectional properties are given in Table 8. All of the arch members are loaded with a concentrated load at the crown (see Fig. 5(a)).

In addition, some results are presented for the lateral buckling of an initially straight I-beam under a uniform dead load. Restraint of warping of the cross-sections is included in the behavior of these particular members. One of the member is a rolled steel section 16 WF 64 and the other is a section especially contrived to demonstrate a particular point. The cross section of this special member is shown in Fig. 6(b).

Unless otherwise noted, all buckling loads are of the bifurcation type as opposed to limit points. The following notation is used in the Figures and Tables.

α = non-dimensionalized load for out-of-plane buckling problems, $\alpha = Pa^2/\sqrt{EI_2 GJ}$

β = non-dimensionalized load for in-plane buckling problems, $\beta = PL^2/EI_1$

H = rise of arch

L = span of arch

I_1 = for a planar member, moment of inertia about an axis perpendicular to plane

I_2 = for a planar member, moment of inertia about the axis in the plane

J = St.-Venant torsion constant

C_w = warping constant

ε_c = strain of centerline of member

5.3. Numerical Results

5.3.1. Prediction of Buckling Loads

Data are given in Table 2 which indicate the rate of convergence of the process of predicting bifurcations. In general, the change of sign of the determinant of the equations expressing the boundary conditions is used to obtain an initial estimate of the buckling load. Then the prediction process is implemented to "home in" on the actual value. As may be seen from the successive values of P and δP in Table 2, it is necessary to apply the procedure taking advantage of orthogonality between the eigenvector and changes in the prebuckling configuration near the buckling load in order to guarantee convergence (see Sec. 4.5.). From Table 2, the case of out-of-plane buckling is seen to converge quite rapidly even though the initial estimate of the buckling load is in error by a factor of more than three. This is to be expected, since the problem is essentially a classical eigenvalue problem. That is, the prebuckling deformations are of relatively slight importance.

The last case given in Table 2 indicates that it is possible to avoid the use of the determinant involving the boundary conditions in isolating the buckling load. In this particular case, an increment of deflection was introduced and then the prediction process implemented far from the actual buckling load. Although the process is seen to converge, it is probably less efficient to start the prediction process this far from the buckling load.

There are some apparent minor discrepancies in Table 2. The errors in the X_3 coordinate of the load, as well as the buckling load itself, are somewhat dependent (in the fourth or fifth significant figures) on the number of integration intervals as well as the number of cycles of the Newton-Raphson technique. Where a direct comparison is made in Table 2 (cases 1 and 2) the integration intervals and number of cycles of Newton-Raphson are the same.

5.3.2. Buckling Loads and Deflections of Simply Supported Arches

Results for the buckling loads and deflections of a few typical simply supported arches are given in Table 3. It is seen that the results agree well with seom of the previous analytical and experimental work. Figures 7 and 8 show both the prebuckling and a part of the postbuckling curve for the simply supported arches. The results plotted are for an inextensional centerline since the effect of extension is negligible for the simply supported arches studied here. From Figs. 7 and 8, it is seen that for H/L equal to 0.50, the load carrying capacity increases after bifurcation. This has been observed experimentally by Langhaar, Boresi and Carver (1954) where, under a concentrated gravity load, the arch did not collapse upon entering the side-sway buckling mode. For H/L = 0.25, the load carrying capacity of the arch decreases rapidly after buckling (see Figs. 7(b) and 8(b)). This agrees with the analytical result of Huddleston (1968). Figures 7(b) and 8(b) indicate that the method can be used to trace as much of the postbuckling configuration as desired.

The data given in Table 3 indicate that the stiffness of a simply supported arch, H/L = 0.50, is slightly reduced when extension of

the centerline is permitted in prebuckling and postbuckling behavior. However, the buckling load for this arch is increased when extension is taken into account. This is not a contradiction of Rayleigh's theorem (1894) since bifurcations from two different prebuckling configurations are being compared and there is no way to assess the effect of the internal constraint ($\varepsilon_c = 0$). This phenomenon of a more flexible structure having a higher buckling load was reported by Masur, Chang and Donnell (1961). In that study, a gable frame with a concentrated load at the peak was analyzed both with and without an inextensible tie connecting the tops of the columns. Removal of the tie results, of course, in large prebuckling deformations, but, paradoxically, increases buckling load. Another instance of this same phenomenon occurs in another part of the present study concerning the out-of-plane buckling of arches which are either simply supported or clamped in the plane. The simply supported arches given significantly higher buckling loads than the clamped ones for the same H/L even though they are more flexible than the latter (see Fig. 10).

For in-plane buckling problems, each cycle of Newton-Raphson required about one second of computer time on an IBM 360-75 system. Usually two additional cycles of Newton-Raphson sufficed to decrease the residuals to less than 0.05 percent of their values computed at the end of the first cycle. In the computations, only two load increments were needed to arrive at the vicinity of the bifurcation point for H/L = 0.25, and three load increments for H/L = 0.50.

5.3.3. Two Dimensional Arches with Clamped Ends

Considerable analytical and experimental work has been done on shallow clamped arches. One of the sample problems in this study was solved for comparison with the experimental work of Gjelsvik and Bodner (1962) and the analytical work of Schreyer and Masur (1966) on shallow arches under concentrated loads. As may be seen from Table 3, the comparison with the results given by Schreyer and Masur is quite good. The agreement with the experimental work of Gjelsvik and Bodner is not as close, but there are uncertainties in the experiments involving support conditions, modulus of elasticity, loading and dead weight of the arch. It is appropriate to point out that Gjelsvik and Bodner recorded the buckling load as a maximum on the experimental load-deflection curve whereas, the buckling load computed here is of the bifurcation type and occurs after the limit point (see Fig. 9(a)) on the load-deflection curve. Schreyer and Masur noted that arches with certain rise-to-span ratios exhibit this phenomenon of bifurcation buckling after P falls off from the value at a limit point. As expected, extension of the centerline is significant for shallow clamped arches, as may be seen from Table 3.

Results are also presented for a rather steep clamped arch (H/L = 0.25) which does not buckle but rather maintains a symmetrical configuration during the loading process (see Fig. 9(b)).

5.3.4. Buckling Loads and Displacements for Three-Dimensional Arches

Table 4 gives non-dimensionalized data for the buckling loads of four sample problems of out-of-plane buckling of initially planar arches.

No results were found in the literature with which to compare these results directly. However, Timoshenko and Gere (1961) present some results for the out-of-plane buckling of a uniformly compressed arch which seem consistent with the results obtained here.

For a given H/L, the simply supported arches have a higher buckling load than the clamped arches, although the clamped arches are initially stiffer. As may be seen from Figs. 10 and 11, all the arch members examined in this study had reserve load carrying capacity after the buckling load was reached.

In Table 5, results are given for an arch with a section devised so that it first buckles in the plane and, upon continued loading, later buckles out-of-plane. To conserve computer time, 40 points on the arch were used in this problem instead of 100 in the numerical integration process. This is the reason for the slight discrepancy between the results presented for this problem and for the two-dimensional problems. Figure 6(a) is a schematic of what the member cross section might be in order to have the required relationships among the three rigidities.

5.3.5. Lateral Buckling of I-Beams

Results are given in Table 6 for the lateral buckling load of a clamped I-beam under a uniform load. As may be seen from Table 6, the result is in excellent agreement with the previous work by Austin, Yegian and Tung (1957). The suppression technique is used here to derive these results. It appears that the lateral buckling analysis of most rolled beams may proceed straightforwardly as an initial value problem without resorting

to use of the suppression technique. Allowable stresses and deflections preclude extremely long members which give rise to numerical difficulties. When the rolled sections are used as arches, however, the loads can be partially supported by normal forces. This makes possible a longer member and increases the effect of unwanted growing solutions during the numerical integration process.

Thus, there are cases in which some technique like suppression is required in order to obtain accurate answers, even with double precision arithmetic. The numerical difficulty arises when the net effect of warping restraint on the torsional stiffness of the whole member is small. In this case, the warping restraint is only an edge effect. A long, slender member is then indicated if a computation is to be carried out to indicate what the consequences of growing solutions might be. The section of Fig. 6(b) was used as a long beam and the lateral buckling load sought. Results are given in Table 6 for the buckling load of the member and are given in Table 7 for a comparison of the behavior of the solution versus the number of suppressions used. As may be seen from Table 7, ten suppressions are sufficient to ensure satisfaction of the boundary conditions while two suppressions lead to diverging approximations.

Although results are not given here, as a matter of curiosity, the beginning of the postbuckling curve for lateral buckling of an I-beam under a uniform load was computed. For the particular member, the load carrying capacity dropped off after buckling. This behavior seems quite reasonable since the lateral buckling is accompanied by rotation of the cross section, bringing the smaller flexural rigidity into prominence.

6. CONCLUSIONS AND RECOMMENDATIONS FOR FURTHER STUDY

6.1. Summary of the Computational Procedures

The methods developed in this study for the analysis of buckling and postbuckling behavior can be summarized as follows. A new method is presented in Chapters 2, 3, and 4 for improving an initial approximation to a bifurcation point on a nonlinear load-deflection curve. In addition, an approximation to the eigenvector is generated and improved simultaneously with the prebuckling configuration. The initial stages of postbuckling are investigated by adding a multiple of the eigenvector to the prebuckling configuration at the onset of buckling. Subsequent postbuckling behavior may be examined by the application of the standard Newton-Raphson procedure as described in Chapter 3.

The numerical methods introduced here for solving buckling and postbuckling problems involve two modifications of the usual Newton-Raphson technique. The first of these modifications extends the Newton-Raphson technique to the simultaneous improvement of eigenvalues and eigenvectors when there is no difficulty in computing changes in the prebuckling configuration accurately. As indicated in Chapter 2, a difficulty occurs, in general, in the vicinity of bifurcation points where the equations specifying changes in the prebuckling configuration become ill-conditioned. A second modification of the usual Newton-Raphson technique has been devised to permit calculation of changes in the prebuckling configuration in the neighborhood of a bifurcation. In this variant of the procedure, the orthogonality relation between the eigenvector and changes in the prebuckling configuration plays an essential role.

6. CONCLUSIONS AND RECOMMENDATIONS FOR FURTHER STUDY

6.1. Summary of the Computational Procedures

The methods developed in this study for the analysis of buckling and postbuckling behavior can be summarized as follows. A new method is presented in Chapters 2, 3, and 4 for improving an initial approximation to a bifurcation point on a nonlinear load-deflection curve. In addition, an approximation to the eigenvector is generated and improved simultaneously with the prebuckling configuration. The initial stages of postbuckling are investigated by adding a multiple of the eigenvector to the prebuckling configuration at the onset of buckling. Subsequent postbuckling behavior may be examined by the application of the standard Newton-Raphson procedure as described in Chapter 3.

The numerical methods introduced here for solving buckling and postbuckling problems involve two modifications of the usual Newton-Raphson technique. The first of these modifications extends the Newton-Raphson technique to the simultaneous improvement of eigenvalues and eigenvectors when there is no difficulty in computing changes in the prebuckling configuration accurately. As indicated in Chapter 2, a difficulty occurs, in general, in the vicinity of bifurcation points where the equations specifying changes in the prebuckling configuration become ill-conditioned. A second modification of the usual Newton-Raphson technique has been devised to permit calculation of changes in the prebuckling configuration in the neighborhood of a bifurcation. In this variant of the procedure, the orthogonality relation between the eigenvector and changes in the prebuckling configuration plays an essential role.

The suppression technique or some equivalent scheme may be necessary when numerical integration procedures are used to solve eigenvalue problems of plate and shell structures. It is well known that the differential equations expressing the behavior of plate and shell structures have edge effects as part of their solution. A technique such as the shooting method would be especially difficult to apply to such problems.

Although the numerical examples were chosen primarily to demonstrate the capabilities of the numerical technique, some interesting behavior of various arches has been found. It appears that in some cases a more flexible structure (in so far as prebuckling deformations are concerned) may have a higher buckling load. This was observed in the in-plane buckling of an initially planar, simply-supported arch under a concentrated load. When extension of the centerline was permitted the buckling load was higher than its counterpart when extension was restrained. Similarly, in the out-of-plane buckling of an initially planar arch, for a given H/L, the simply supported arches had a higher buckling load than the clamped arches. The effectiveness of the numerical techniques is indicated in a particularly striking manner by the somewhat artificial problem of the special arch member discussed in Chapter 5 which buckled in its plane first and subsequently out-of-plane. No difficulty was experienced in following this complex load-deflection path.

6.3. Recommendations for Further Study

The proposed method may be applied to many practical problems of technical interest. Buckling and vibrations of thin curved members where

initial stresses are present can be treated with minor changes in the computer codes developed in this study. In addition, nonlinear stress-strain laws could be admitted where the problem precludes significant unloading.

The method may also be extended to eigenvalue problems in plate and shell type structures. The general procedure is unchanged. However, the linearized problems must be treated by a technique for approximate solution of linear partial differential equations, rather than ordinary differential equations.

Certain eigenvalue problems in gyroscopic motion may also be solved, as is obvious from Kirchhoff's kinetic analogue and the general theory developed here (see Kirchhoff (1859) and Love (1927)).

The problem of deciding which boundary condition to relax when generating the approximate eigenvector needs more study. A sure, but somewhat inelegant, solution to this difficulty is suggested in Section 4.6.

LIST OF REFERENCES

Austin, W. , Yegian, S., and Tung, T. P., 1955, "Lateral Buckling of Elast. ally End-Restrained I-Beams," Transactions of the American Society of Civil Engineers, Vol. 122, 1957.

Berezin, I. S., and Zhidkov, N. P., 1960, Computing Methods, Vol. 2, Pergamon Press, 1965 (translated from the Russian edition of 1960).

Bueckner, H. F., Johnson, M. W., Jr., and Moore, R. J., 1965, "The Calculation of Equilibrium States of Elastic Bodies by Newton's Method," Proceedings of the Ninth Midwestern Mechanics Conference, University of Wisconsin, Madison, August, 1965.

Chen, C. S., and Boresi, A. P., 1961, "Effect of Certain Approximations Upon the Theoretical Buckling of Circular Rings and Arches," Proceedings of the Seventh Midwestern Mechanics Conference, Michigan State University, East Lansing, September, 1961.

Clebsch, A., 1862, "Theorie der Elasticitat fester Korper," Leipzig, 1862.

Cohen, G. A., 1965, "Computer Analysis of Asymmetric Free Vibrations of Ring-Stiffened Orthotropic Shells of Revolution," Journal of the American Institute of Aeronautics and Astronautics, December, 1965.

Crandall, S. H., 1956, Engineering Analysis, McGraw-Hill Book Company, Inc., New York, 1956.

Donnell, L. H., 1934, "A New Theory for the Buckling of Thin Cylinders Under Axial Compression and Bending," Transactions of the American Society of Mechanical Engineers, Vol. 56, 1934.

Galletly, G. D., Kyner, W. T., and Moller, C. E., 1961, "Numerical Methods and the Bending of Ellipsoidal Shells," Journal of the Society for Industrial and Applied Mathematics, June, 1961.

Gjelsvik, A., and Bodner, S. R., 1962, "Energy Criterion and Snap Buckling of Arches," Journal of the Engineering Mechanics Division, Proceedings of the American Society of Civil Engineers, October, 1962.

Goldberg, J. E., Setlur, A. V., and Alspaugh, D. W., 1965, "Computer Analysis of Non-Circular Cylindrical Shells," Symposium on Shell Structures, International Association for Shell Structures, Budapest, Hungary, September, 1965.

Holzer, H., 1921, Die Berechnung der Drehschwingungen, Springer-Verlag, Berlin, 1921. Republished by Edwards Bros., Publisher, Inc., Ann Arbor, Michigan, 1948.

Huddleston, J. V., 1968, "Finite Deflections and Snap-Through of High Circular Arches," Journal of Applied Mechanics, December, 1968.

Jordan, P. F., and Shelley, P. E., 1966, "Stabilization of Unstable Two-Point Boundary Value Problems," Journal of the American Institute of Aeronautics and Astronautics, May, 1966.

Kalnins, A., 1964, "Free Vibrations of Rotationally Symmetric Shells," Journal of the Acoustical Society of America, July, 1964.

Kalnins, A., and Lestingi, J. F., 1967, "On Nonlinear Analysis of Elastic Shells of Revolution," Journal of Applied Mechanics, March, 1967.

Kerr, A. D., and Soifer, M. T., 1969, "The Linearization of the Prebuckling State and Its Effect on the Determined Instability Loads," Journal of Applied Mechanics, December, 1969.

Kirchhoff, G., 1859, "Uber das Gleichgewicht und die Bewegung eines unendlich dünnen elastichen Stabes," J. f. Math. (Crelle), Bd. 56 (1859).

Koiter, W. T., 1945, "On the Stability of Elastic Equilibrium," Thesis, Polytechnic Institute Delft, H. J. Paris, Amsterdam, Translated from the Dutch by O. W. Leiberger Research Laboratories, Inc., NASA TT F-10, 833, March, 1967.

Langhaar, H. L., Boresi, A. P., and Carver, D. R., 1954, "Energy Theory of Buckling of Elastic Rings and Arches," Proceedings of Second U. S. National Congress of Applied Mechanics, University of Michigan, Ann Arbor, June, 1954.

Leicester, R. H., 1968, "Finite Deformations of Shallow Shells," Journal of the Engineering Mechanics Division, Proceedings of the American Society of Civil Engineers, December, 1968.

Love, A. E. H., 1927, A Treatise on the Mathematical Theory of Elasticity, 4th Ed., Macmillan Company, London, 1927. Republished by Dover Publications, Inc., 1944.

Masur, E. F., Chang, I. C., and Donnell, L. H., 1961, "Stability of Frames in the Presence of Primary Bending Moments," Journal of the Engineering Mechanics Division, Proceedings of the American Society of Civil Engineers, August, 1961.

Rall, L. B., 1961, "Newton's Method for the Characteristic Value Problem $A X = \lambda B X$," Journal of the Society for Industrial and Applied Mathematics, June, 1961.

Rayleigh, Lord, 1894, Theory of Sound, 2nd Ed., Vol. 1, Macmillan Company, London, 1894. Republished by Dover Publications, Inc., 1945.

Routh, E. J., 1905, Dynamics of a System of Rigid Bodies, 6th Ed., Macmillan Company, London, 1905. Republished by Dover Publications, Inc., 1955.

Schmidt, R., 1969, Discussion of "The Strongest Circular Arch - A Perturbation Solution" by C. H. Wu, Journal of Applied Mechanics, September, 1968, in Journal of Applied Mechanics, December 1969.

Schreyer, H. L., and Masur, E. F., 1966, "Buckling of Shallow Arches," Journal of the Engineering Mechanics Division, Proceedings of the American Society of Civil Engineers, August, 1966.

Thurston, G. A., 1969, "Continuation of Newton's Method Through Bifurcation Points," Journal of Applied Mechanics, September, 1969.

Timoshenko, S. P., and Gere, J. M., 1961, Theory of Elastic Stability, McGraw-Hill Book Company, Inc., New York, 1961.

von Kafmań, T., and Tsien, H. S., 1939, "The Buckling of Spherical Shells by External Pressure," Journal of the Aeronautical Sciences, December, 1939.

Vlasov, V. Z., 1959, Thin-Walled Elastic Beams, U. S. Dept. of Commerce, PST Cat. No. 428, 1961 (Translation of the Russian Edition of 1959).

West, H. H., and Robinson, A. R., 1968, "Continuous Method of Suspension Bridge Analysis," Journal of the Structural Division, Proceedings of the American Society of Civil Engineers, December, 1968.

Zarghamee, M. S., and Robinson, A. R., 1967, "A Numerical Method for Analysis of Free Vibration of Spherical Shells," Journal of the American Institute of Aeronautics and Astronautics, July, 1967.

Ziegler, H., 1956, "On the Concept of Elastic Stability," Advances in Applied Mechanics, Vol. 4, Academic Press Inc., New York, 1956.

TABLE 1. INITIAL VALUES AND RESIDUALS FOR CLAMPED ARCH

Quantity	Homogeneous Solutions							Particular Solution
	1	2	3	4	5	6	7	8
δN_1	1	0	0	0	0	0	0	0
δN_2	0	1	0	0	0	0	0	0
δN_3	0	0	1	0	0	0	0	0
δM_1	0	0	0	1[a]	0	0	0	0
δM_2	0	0	0	0	1	0	0	0
δM_3	0	0	0	0	0	1	0	0
δP	0	0	0	0	0	0	1[b]	0
Right-Hand-Sides of Linearized Equations	0	0	0	0	0	0	0	R

[a] Corresponding initial incremental curvatures are computed by use of Eq. (3.14)

[b] Not really an initial value since it enters the computations at concentrated load in middle of member (Eq. (3.14))

TABLE 2. PREDICTION OF BUCKLING LOADS

Buckling Type	P, lb.	δP, lb.	Error in X_3 Coordinate of Load, in.	Orthogonality Imposed	H/L
in-plane	219390		.00038		
	216769	-2621	.65824	no	.25
	216791	22	.00000		
	217864	893	.06304		
	216850	-834			
in-plane	219390		.0002		
	216769	-2621	.00021	yes	.25
	216791	22	.00039		
		0			
in-plane	97318		.00335	yes	.50
	97806	488	.00400		
		2			
out-of-plane	237.99		.00042		
	783.33	545.33	.00047	yes[a]	.50
		.23			
in-plane	157450		.00105		
	199272	41822	.00003	yes	.25
	215425	16153	.00360		
	216772	1348	.00691		
		-9			

[a] Automatically satisfied since in-plane prebuckling configuration is orthogonal to out-of-plane eigenvector.

TABLE 3. IN-PLANE BUCKLING LOADS OF ARCHES

Boundary Conditions	Extension of Centerline	H/L	Pa^2/EI_1	d_2/L	Source
Simply Supported	yes	.25	12.981	.06815	present
Simply Supported	no	.25	13.006	.06727	present
Simply Supported	no	.25	13.05	----	b
Simply Supported	no	.25	13.0	----	c
Simply Supported	yes	.50	5.8703	.09768	present
Simply Supported	no	.50	5.8685	.09746	present
Simply Supported	yes[a]	.50	6.54	----	c
Simply Supported	yes	.50	6.15	----	c (experiment)
Simply Supported	yes[a]	.50	5.6	----	e
Simply Supported	no	.50	5.86	----	b
Clamped	yes	.044	71.866	.02565	present
Clamped	no	.044	77.777	.02206	present
Clamped	yes	.044	72.2	----	f
Clamped	yes	.044	63.7	----	g (experiment)

[a] Extension of the centerline was permitted in deriving the prebuckling configuration, but not in the eigenvector.

[b] Schmidt (1969)

[c] Huddleston (1967)

[d] Langhaar, Boresi, and Carver (1954)

[e] Chen and Boresi (1961)

[f] Schreyer and Masur (1966)

[g] Gjelsvik and Bodner (1962)

TABLE 4. OUT-OF-PLANE BUCKLING LOADS AND DISPLACEMENTS FOR SIMPLY SUPPORTED AND CLAMPED ARCHES

H/L	Clamped		Simply-Supported	
	Pa^2/EI_2 GJ	d_2/a	Pa^2/EI_2 GJ	d_2/a
0.25	3.453	0.0007857	3.952	0.001389
0.50	0.6684	0.0003262	0.7701	0.0006080

TABLE 5. BUCKLING LOADS AND DEFLECTIONS FOR A SIMPLY-SUPPORTED ARCH WHICH FIRST BUCKLES IN-PLANE AND UPON INCREASED LOADING BUCKLES OUT-OF-PLANE, H/L = 0.25, $\varepsilon_c = 0$

In-plane Buckling		Subsequent Out-of-Plane Buckling		
Pa^2/EI_1	d_2/L	Pa^2/EI_1	d_2/L	d_3/L
13.04[a]	0.06648	12.70	0.07851	0.3562

[a]This differs from the results for the in-plane buckling of other two dimensional arches because fewer points were used here in the numerical integration process.

TABLE 6. LATERAL BUCKLING LOADS OF UNIFORMLY LOADED, CLAMPED I-BEAMS

Member	L, in.	I_1, in.^{4}	I_2, in.^{4}	J, in.^{4}	C_w, in.^{6}	P_{cr}, lb/in	Source	No. of Suppressions
16WF64	504	864	68.4	2.5	3850	324.11	present	2[a]
16WF64	504	864	68.4	2.5	3850	325.	b	---
Special (See Fig. 6b)	228	146.2	2.08	2.5	52.0	456.21	present	10

[a]Ten suppressions gave the same buckling load to five significant figures

[b]Austin, Yegian, and Tung (1957)

TABLE 7. USE OF SUPPRESSION TO ENSURE ACCURATE BUCKLING LOADS OF I-SHAPED MEMBERS

p, lb/in.	W, lb/in.	No. of Suppressions
454.81	1.40	10
456.21	----	
454.81	111.93	2
566.73	2278.04	
2844.77	------	

TABLE 8. MEMBER SECTION PROPERTIES

Out-of-plane buckling (12WF31)	$I_1 = 238.4\ in^4$, $I_2 = 19.8\ in^4$, $J = .5065\ in^4$
In-plane buckling of simply supported arches	$I_1 = 18.0\ in^4$, Area = $6.0\ in^2$
In-plane buckling of clamped arches	$I_1 = .5493 \times 10^{-3}\ in^4$, Area = $.1875\ in^2$

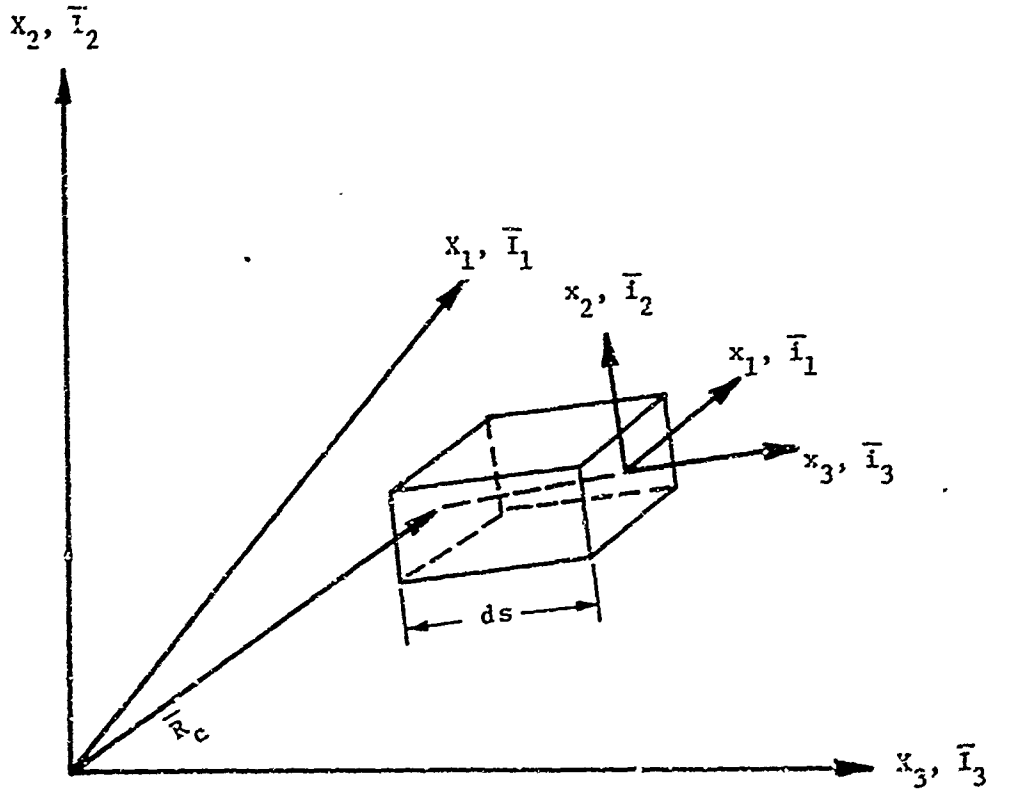

FIG. 1. GLOBAL AND LOCAL COORDINATE SYSTEMS

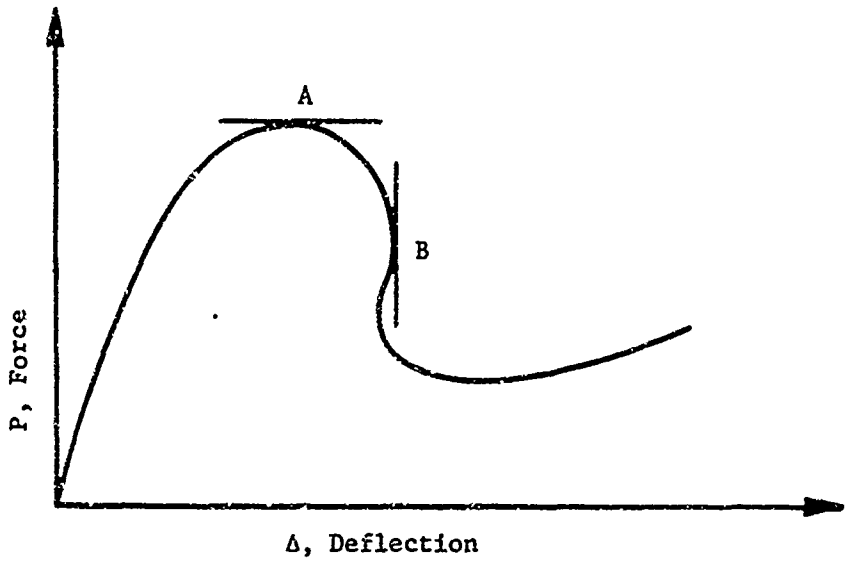

FIG. 2. QUALITATIVE FORCE-DEFLECTION CURVE

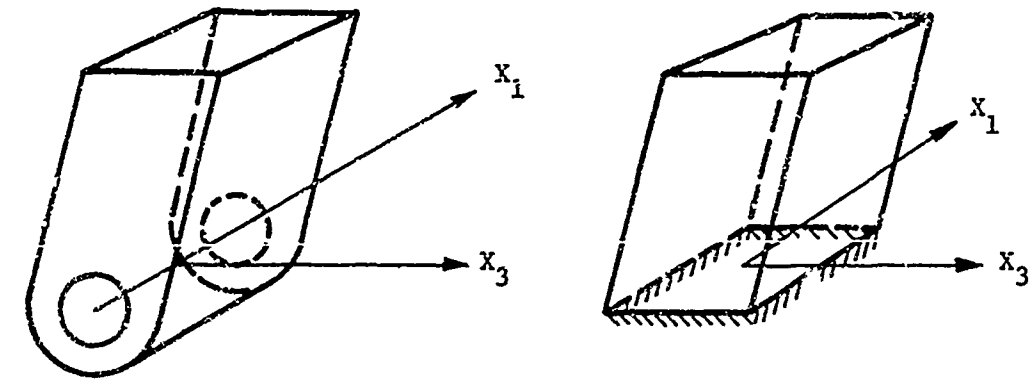

(a) Simple Support (b) Clamped Support

FIG. 3. TYPES OF SUPPORTS FOR ARCH MEMBERS

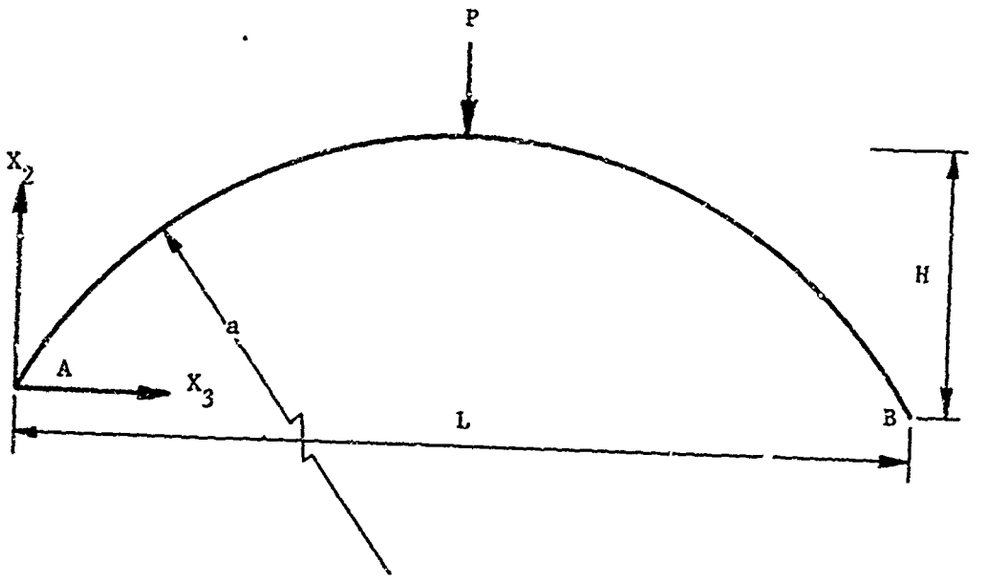

FIG. 4. TYPICAL ARCH MEMBER

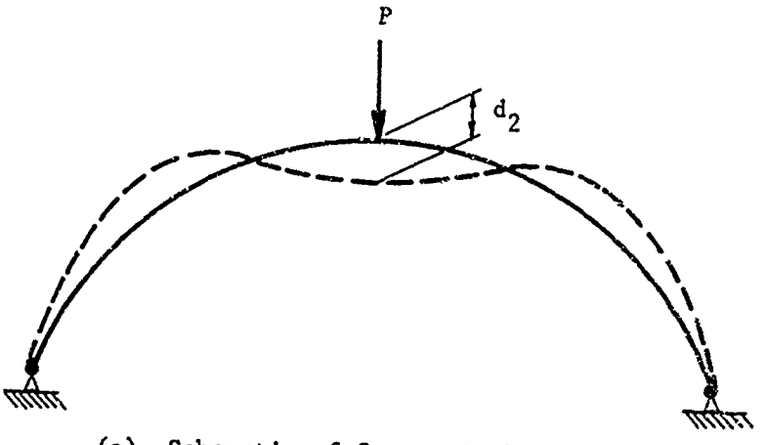

(a) Schematic of Symmetrical Prebuckling Configuration

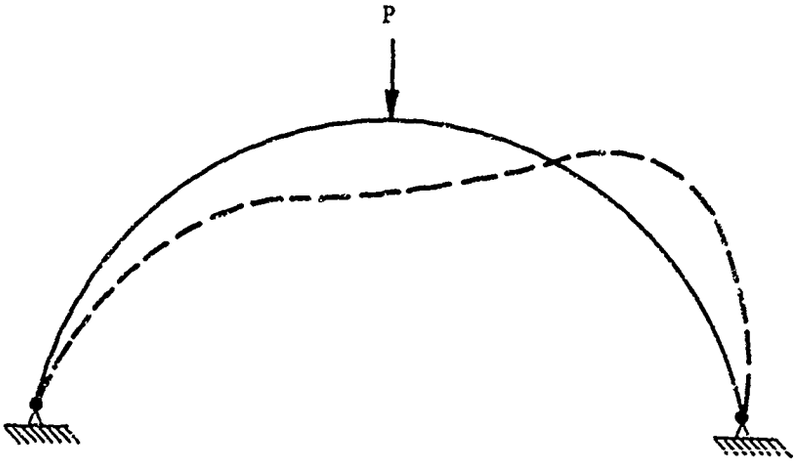

(b) Schematic of Anti-Symmetrical In-plane Buckling Mode

FIG. 5. TYPICAL IN-PLANE BEHAVIOR OF SIMPLY SUPPORTED ARCH

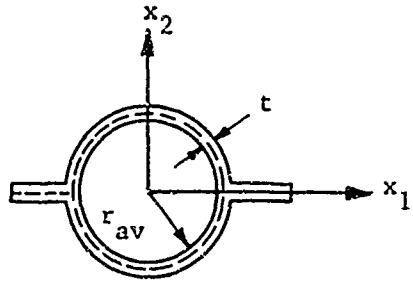

$$I_1 = \pi r_{av}^3 t/2$$

$$J = 2I_1$$

$$I_2 = 1.444I_1$$

(a) Schematic of Cross-Section for Member Which Buckles In-Plane and Then Out-of-Plane

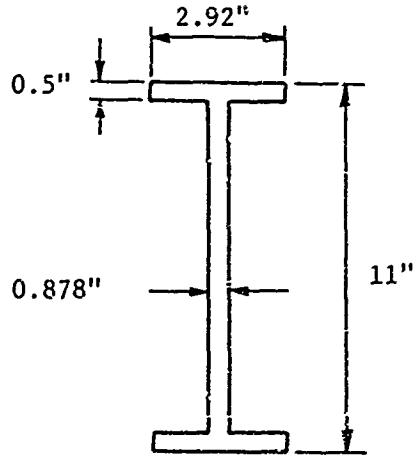

(b) Schematic of Cross-Section for Special Member in Lateral Buckling Study

FIG. 6. SPECIAL CROSS SECTIONS OF MEMBERS USED IN THE ANALYSIS

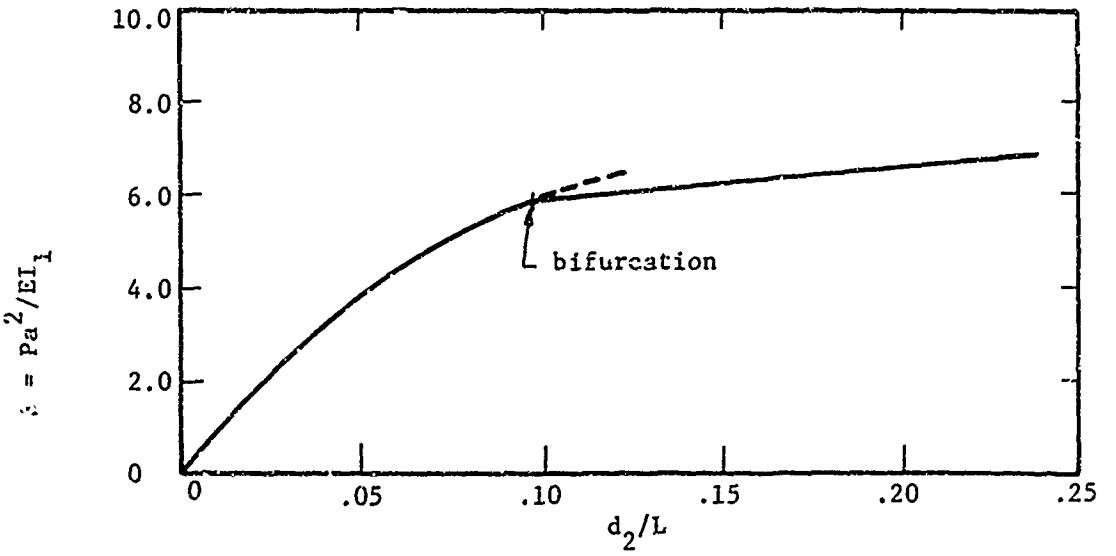

(a) H/L = .50

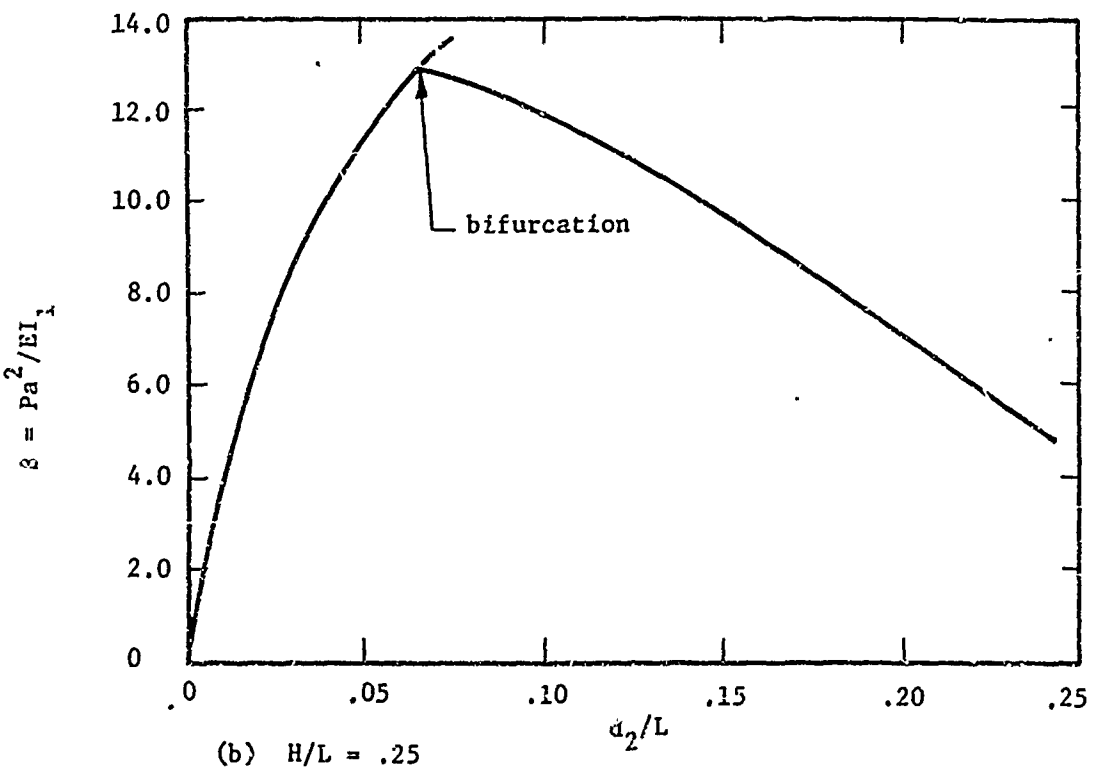

(b) H/L = .25

FIG. 7. LOAD VERSUS VERTICAL DEFLECTION AT CROWN, IN-PLANE BUCKLING OF SIMPLY SUPPORTED ARCHES, $\varepsilon_c = 0$

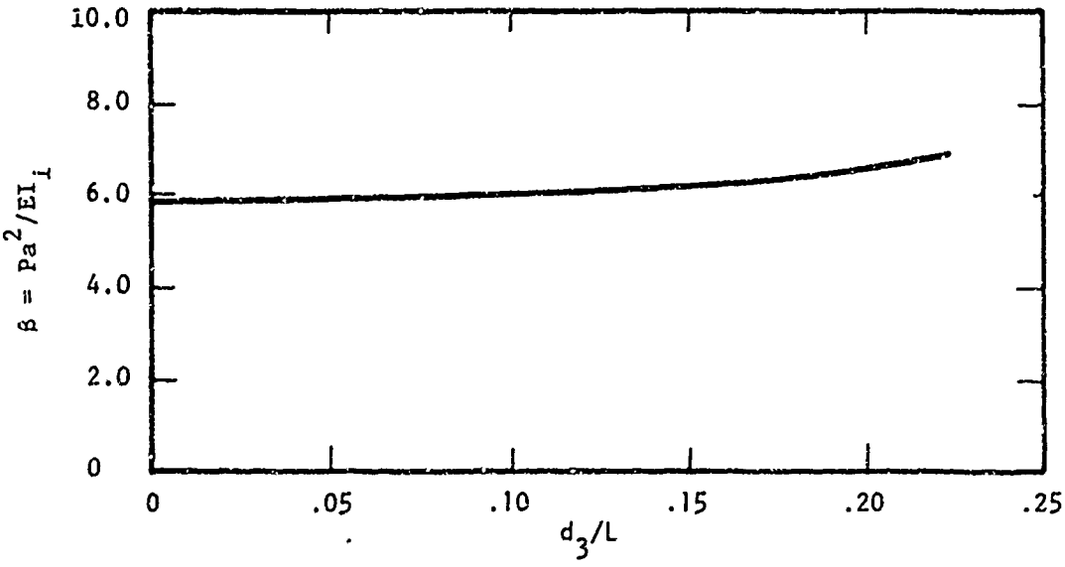

(a) H/L = .50

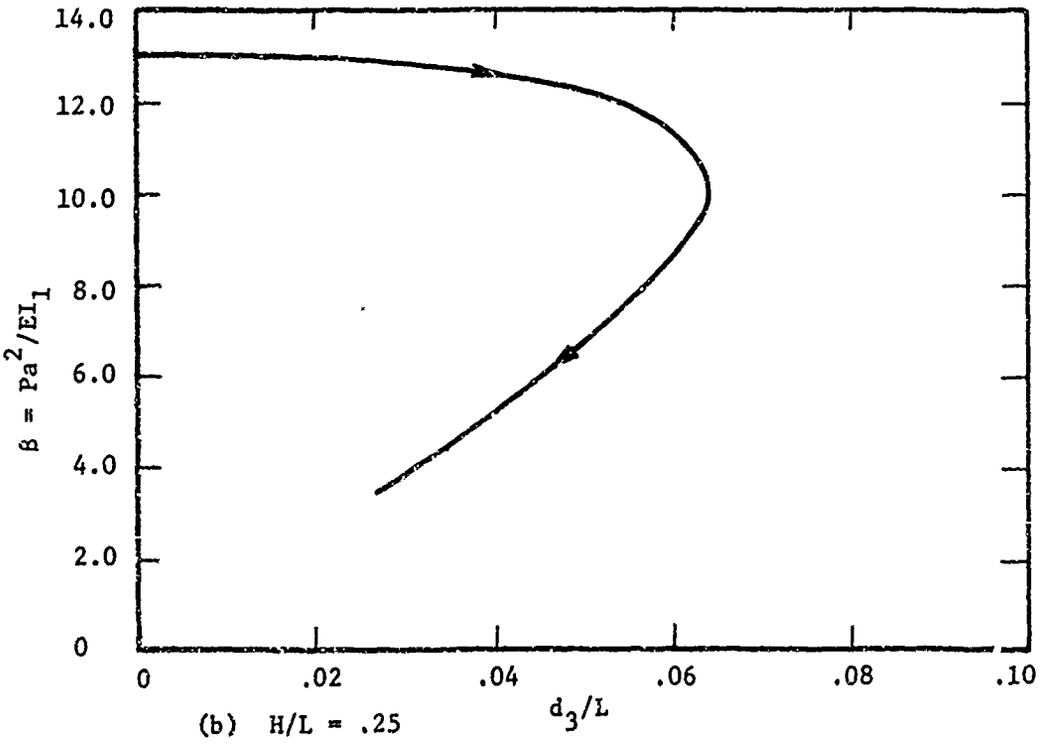

(b) H/L = .25

FIG. 8. LOAD VF 'US HORIZONTAL DEFLECTION AT CROWN, IN-PLATE BUCKLING OF SIMPLY SUPPORTED ARCHES, $\varepsilon_c = 0$

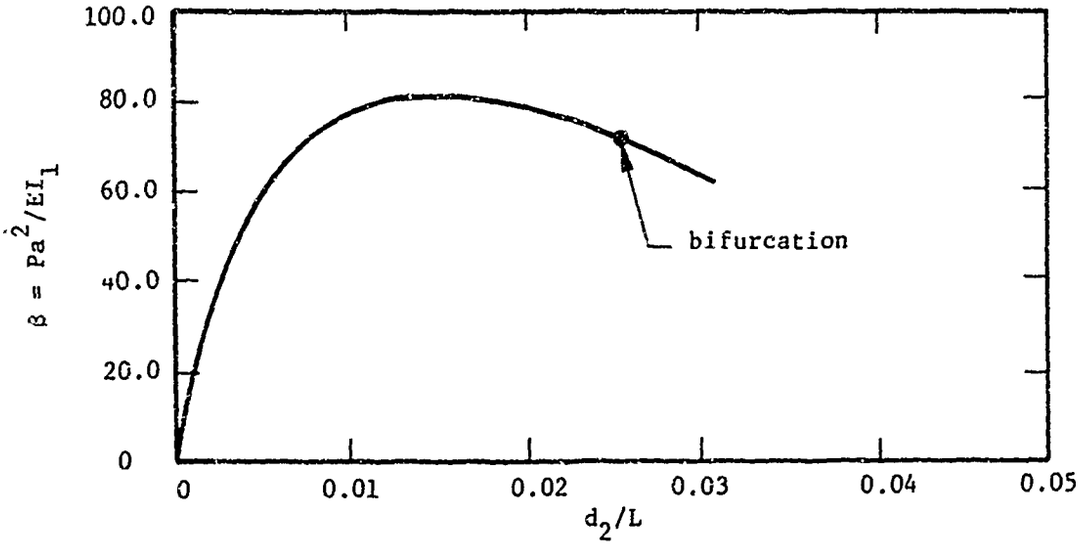

(a) H/L = .0446

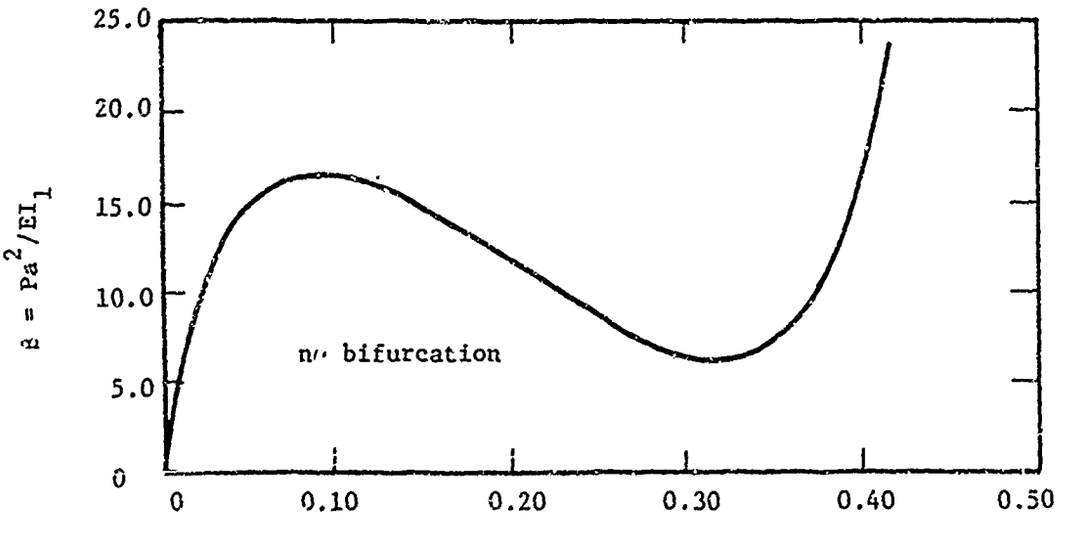

(b) H/L = .25

FIG. 9. LOAD VERSUS VERTICAL DEFLECTION AT CROWN, IN-PLANE BUCKLING OF CLAMPED ARCHES

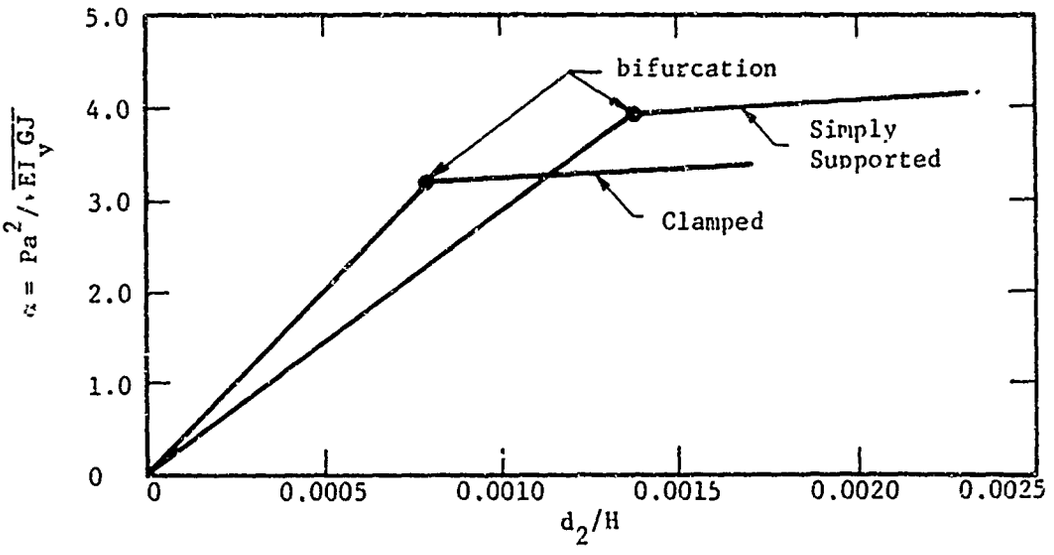

(a) H/L = .25

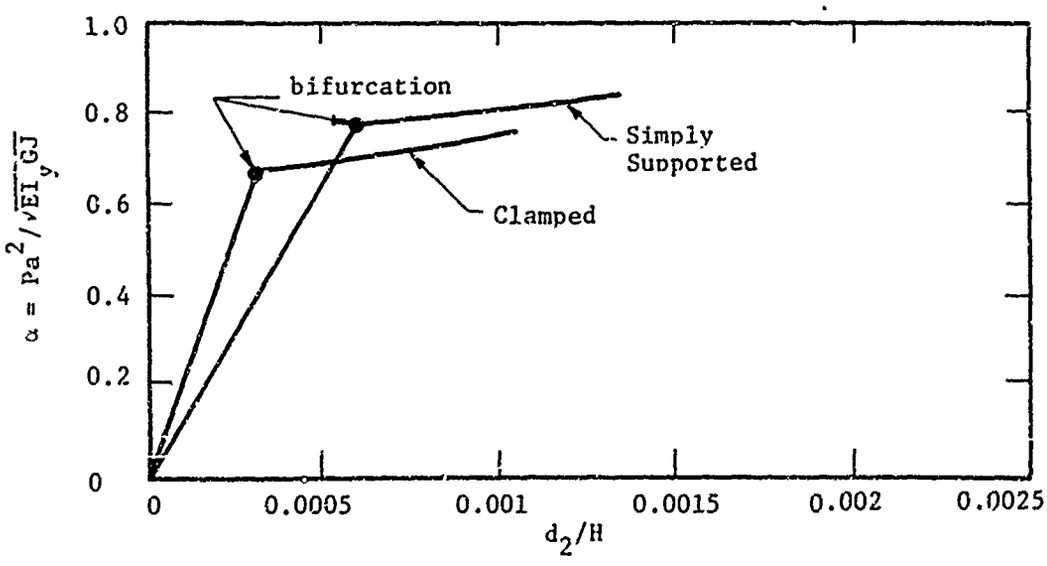

(b) H/L = .5

FIG. 10. LOAD VERSUS VERTICAL DEFLECTION AT CROWN, OUT-OF-PLANE BUCKLING OF CLAMPED AND SIMPLY SUPPORTED ARCHES, $\epsilon_c = 0$

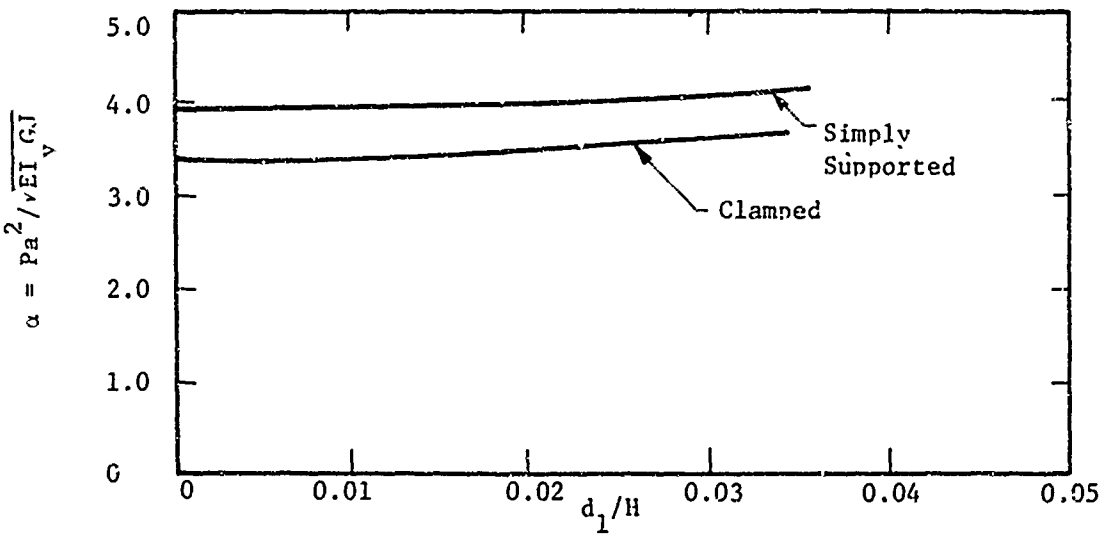

(a) H/L = .25

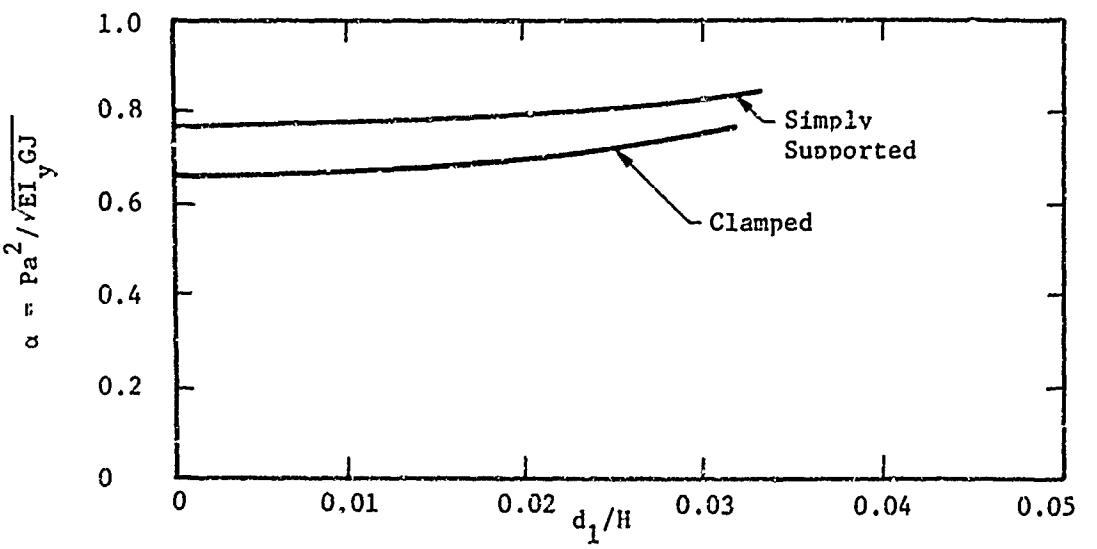

(b) H/L = .5

FIG. 11. LOAD VERSUS OUT-OF-PLANE DEFLECTION AT CROWN, OUT-OF-PLANE BUCKLING OF CLAMPED AND SIMPLY SUPPORTED ARCHES, $\epsilon_c = 0$

APPENDIX A

SOLVABILITY OF THE BASIC EQUATIONS OF THE METHOD

A.1. Case of a Single Root

Consider the method proposed in Chapter 2 as applied to the determination of the bifurcation point and corresponding eigenvector of the algebraic system

$$A\,X = \lambda\,B\,X \tag{A.1}$$

where for purposes of this discussion, A, B, and λ correspond to the onset of buckling. At buckling, both A and B are assumed to be self-adjoint and B is taken to be positive definite. The side condition, corresponding to Eq. (2.6) is taken as

$$X^T\,B\,\delta X = 0 \tag{A.2}$$

At the buckling point, the coefficient matrix given by the left-hand-side of Eq. (2.3) and Eq. (A.2) is

$$C = \begin{bmatrix} A - \lambda_{cr}B & \vdots & -B\,x_1 \\ \cdots & \cdots & \cdots \\ -x_1^T\,B & \vdots & 0 \end{bmatrix} \tag{A.3}$$

where λ_{cr} is the buckling load and x_1 is the corresponding eigenvector.

The basic method will fail if the coefficient matrix C of Eq. (A.3), used in the computation of the increments of an approximate eigenvalue and

eigenvector, is singular. It is expected that if this occurs, the singularity will exist at exactly the prebuckling configuration given by A, B, and λ_{cr}. If the order of the original problem is of order n, then C in Eq. A.3 is a symmetrical matrix of order n+1.

The matrix C in Eq. A.3 will now be shown to be nonsingular by a consideration of the eigenvalues of the auxiliary system

$$C\,y = \bar{\lambda}\ D\,y \tag{A.4}$$

where

$$D = \begin{bmatrix} \bar{B} & \vdots & 0 \\ \cdots & \cdots & \cdots \\ 0 & \vdots & 1 \end{bmatrix} \tag{A.5}$$

It may be verified by direct substitution that the eigenvectors y_m, $(m = 1, \ldots\ldots n + 1)$ of the system given by Eq. A.4 are

$\begin{Bmatrix} x_1 \\ \hline 1 \end{Bmatrix}$, $\begin{Bmatrix} x_1 \\ \hline -1 \end{Bmatrix}$, $\begin{Bmatrix} x_k \\ \hline 0 \end{Bmatrix}$, $(k = 2, \ldots\ldots n)$ where the x_1 and x_k are eigenvectors of Eq. (A.1). The corresponding eigenvalues $\bar{\lambda}$ of Eq. (A.4) are 1, +1, and $(\lambda_k - \lambda_{cr})$. The eigenvectors of Eq. (A.1) are found by considering A and B constant at the prebuckling configuration corresponding to the onset of buckling, and are assumed to be normalized with respect to B.

It is not difficult to show that the determinant of C is equal to the product of the $\bar{\lambda}$'s multiplied by det (D). Since the latter is equal to det (B) which is positive, then det (C) is nonzero provided none of the $\bar{\lambda}$ are zero. Only in the case of a multiple root can a $\bar{\lambda}$ be zero. Thus, if

there are no multiple eigenvalues of the original system given by Eq. (A.1), the basic method proposed encounters no numerical difficulties associated with a singularity of C.

A.2. Case of a Double Root

The existence of a double root of Eq. (A.1) (say $\lambda_{cr} = \lambda_K$) implies that the matrix C in Eq. (A.3) is singular at the bifurcation point. This singularity may be removed by the following computational sequence. Two independent eigenvectors are generated by specifying two side conditions for each eigenvector. The two eigenvectors are denoted here by x_1 and x_K and their increments by δx_1 and δx_K. The side conditions for δx_1 are

$$x_K^T B \, \delta x_1 = 0 , \quad x_1^T B \, \delta x_1 = 0 \tag{A.6}$$

and the side conditions for δx_K are

$$x_K^T B \, \delta x_K = 0 , \quad x_1^T B \, \delta x_K = 0 \tag{A.7}$$

The specification of the two side conditions results in the following coefficient matrix for the equations determining the incremental changes in the two eigenvectors

$$\bar{C} = \left[\begin{array}{c|c} C & \\ \hline x_K^T B & 0 \end{array}\right] = \left[\begin{array}{c} C \\ \hline y_K^T D \end{array}\right] \tag{A.8}$$

where D is given by Eq. (A.5), C is given by Eq. (A.3), and $y_K = \left\{ \frac{x_K}{0} \right\}$. The coefficient matrix $\bar{C}$ has one more row than column, but as indicated by Koiter (1945), the equations which give rise to $\bar{C}$ are all valid at the bifurcation point. An independent set of equations with a nonsingular coefficient matrix may be derived by premultiplying $\bar{C}$ by $\bar{C}^T$. The result of this multiplication, which amounts to an application of a least squares technique, is

$$\bar{C}^T\bar{C} = C^T C + D\, y_K y_K^T D \tag{A.9}$$

The object is to show that the coefficient matrix in Eq. (A.9) is nonsingular. The eigenvector y_K corresponds to a zero eigenvalue of the matrix C of Eq. (A.4). As shown in Section A.1, the remaining eigenvalues of C are nonzero. The matrix $C^T C$ in Eq. (A.9) has the same eigenvectors as C. It follows that the eigenvalues of $C^T C$ are the squares of those of C. Now consider the matrix $G = D y_K y_K^T D$ in Eq. (A.9). Direct substitution yields the result

$$G\, y_K = 1\, D\, y_K \tag{A.10}$$

From Eq. (A.10) it may be seen that the eigenvector y_K is also an eigenvector of G and the corresponding eigenvalue is unity. The matrix G is constructed in such a way that its remaining eigenvalues are zero since it is a symmetric matrix of rank one. The remaining eigenvectors of G may therefore be taken the same as those of C.

Thus both matrices C^TC and $Dy_Ky_K^TD$ in Eq. (A.9) have the same eigenvectors. The eigenvalue of the sum of two matrices having the same eigenvectors is merely the sum of the eigenvalues of the individual matrices. It follows that the eigenvalues of $\overline{C}^T\overline{C}$ are those of C^TC except for the zero eigenvalue which becomes + 1 (from the matrix $Dy_Ky_K^TD$). Since all the eigenvalues of $\overline{C}^T\overline{C}$ are nonzero, it is nonsingular and the method proceeds without difficulty.

APPENDIX B

SOLVABILITY OF THE EQUATIONS USED IN DETERMINING ACCURATE CHANGES IN THE PREBUCKLING CONFIGURATION NEAR A BIFURCATION POINT

The linearized operator used to compute changes in the prebuckling configuration becomes singular at bifurcation points, as has been noted by Thurston (1968). This singular operator is denoted here by $\bar{D}$ where

$$\bar{D} = A - \lambda_{cr} B \tag{B.1}$$

The discussion here will be limited to the algebraic eigenvalue problem so that A and B are matrices which define the prebuckling configuration at the onset of buckling and, λ_{cr} is the buckling load. The matrices A and B are assumed to be self-adjoint and B is taken to be positive definite.

A technique has been discussed in Chapter 2 for removing the singularity from $\bar{D}$. It is the object of this Appendix to show that the resulting coefficient matrix is indeed nonsingular. As indicated in Chapters 2, 3, and 4, a side condition is appended to the basic system. This side condition specifies that changes in the prebuckling configuration are orthogonal to the eigenvector and may be expressed formally as

$$x_1^T B y = 0 \tag{B.2}$$

where x_1 is the eigenvector corresponding to the singularity of D and y is the change in the prebuckling configuration. This side condition leads to a new coefficient matrix $\tilde{D}$ given by

$$\tilde{D} = \begin{bmatrix} A - \lambda_{cr} B \\ \hline x_1^T B \end{bmatrix} \tag{B.3}$$

which has one more row than column. As mentioned in Chapter 2, all these equations giving rise to $\tilde{D}$ are valid at the bifurcation point.

A consistent set of equations with a nonsingular coefficient matrix is derived using the least squares technique:

$$\tilde{D}^T\tilde{D} = (A - \lambda_{cr} B)^T (A - \lambda_{cr} B) + Bx_1x_1^T B \tag{B.4}$$

The matrix given in Eq. (B.4) may be shown to be nonsingular by an argument exactly parallel to that given in Appendix A, Section A.2 for the case of a double eigenvalue.

APPENDIX C

ENSURING ORTHONORMALITY OF THE DIRECTION COSINES

The particular technique used in this study for handling the geometry treats each of the nine direction cosines as an independent quantity during certain stages of the numerical computations. Since the direction cosines are required to form an orthonormal set, it is necessary to enforce this constraint in some manner. The method for ensuring orthonormality of the direction cosines is outlined below.

Orthonormality of a set of direction cosines U requires that

$$U\,U^T = I \tag{D.1}$$

where I is the identity matrix. Substitution of an approximately orthonormal set of direction cosines, U_a, into Eq. (D.1) yields

$$U_a U_a^T = I + e\,S \tag{D.2}$$

where S is a symmetric error matrix whose individual elements are presumed to be of order unity and e is small. A correction matrix C is introduced such that

$$U + C = U_a \tag{D.3}$$

The matrix C is, of course, not unique. A convenient choice is

$$C = 1/2\ e\ S\ U \tag{D.4}$$

By direct substitution, it may be shown that Eqs. (D.3) and (D.4) satisfy Eq. (D.2) to terms of order e^2. Since the quantity U in Eq. (D.4) is not known, U_a is used as a first approximation to U. Equation (D.4) becomes

$$C \simeq 1/2 \; e \; S \; U_a \tag{D.5}$$

Equation (D.3) may be used to describe an iterative process where U is interpreted as the latest approximation and U_a as the previous approximation to the required orthonormal set. Substitution of Eq. (D.5) into Eq. (D.3) and rearrangement yields

$$U = (I - 1/2 \; e \; S) \; U_a \tag{D.6}$$

At a particular iterative step, the value of U computed in Eq. (D.6) becomes U_a for the next step. When the coefficient e becomes small enough, the correction process is terminated. This correction process is necessary at each integration point along the member.

The correction process discussed above results in a new set of direction cosines which is n t derivable from the first derivatives, i.e.,

$$\int \left(\frac{d\ell_{ij}}{ds}\right) ds \neq \ell_{ij}, \; (i, j = 1, 2, 3) \tag{D.7}$$

The following computational scheme was devised to ensure that Eq. (D.7) is satisfied. The corrected direction cosines are substituted into Eqs. (3.3) and new first derivatives computed. A quadrature of these first derivatives yields new direction cosines consistent with Eq. (D.7).

Residuals are computed from Eqs. (3.3) using the direction cosines from the quadrature. The residuals are then used to drive the linearized geometric equations of Chapter 3.

This technique has been implemented as part of the solution of the geometric equations of Chapter 3. Before this technique was devised, it was not possible to achieve global equilibrium even though the residuals in the differential equations were small.

The effect of the technique is to transfer the residuals in Eq. (D.2) back to the geometric differential equations, those of Chapter 3. That is, a residual of order e in the algebraic equations results in a residual of order e in the differential equations. The application of Newton-Raphson to the differential equations gives rise to changes of order e in the direction cosines leading to new residuals of order e^2 in the direction cosines.

14 KEY WORDS	LINK A		LINK B		LINK C	
	ROLE	WT	ROLE	WT	ROLE	WT
Arches						
Bifurcations						
Buckling						
Eigenvalues						
Nonlinear Analysis						
Numerical Methods						
Postbuckling						

Unclassified

Security Classification

DOCUMENT CONTROL DATA - R & D

Security classification of title, body of abstract and indexing annotation must be entered when the overall report is classified)

ORIGINATING ACTIVITY (Corporate author) University of Illinois Department of Civil Engineering Urbana, Illinois	2a. REPORT SECURITY CLASSIFICATION Unclassified 2b. GROUP

3 REPORT TITLE

Numerical Methods for the Analysis of Buckling and Postbuckling Behavior of Arch Structures

4 DESCRIPTIVE NOTES (Type of report and, inclusive dates)

Report

5 AUTHOR(S) (First name, middle initial, last name)

John F. Harris and Arthur R. Robinson

6 REPORT DATE	7a. TOTAL NO. OF PAGES	7b. NO. OF REFS
September 1970	86	35

8a. CONTRACT OR GRANT NO N00014-67-A-0305-0010 b. PROJECT NO c. d.	9a. ORIGINATOR'S REPORT NUMBER(S) Civil Engineering Studies, Structural Research Series No. 364 Department of the Navy 9b. OTHER REPORT NO(S) (Any other numbers that may be assigned this report)

10 DISTRIBUTION STATEMENT

Qualified requester may obtain copies of this report from DDC

11. SUPPLEMENTARY NOTES	12. SPONSORING MILITARY ACTIVITY
	Office of Naval Research Structural Mechanics Branch

13. ABSTRACT

The object of this study is to develop numerical methods for the analysis of structures having prebuckling configurations which are nonlinear functions of the loading parameter.

A set of numerical procedures is presented for the simultaneous improvement of an approximate eigenvector and of an approximate location of a bifurcation point on the load-deflection curve. These methods include a technique for determining accurately the changes in the prebuckling configuration near bifurcation points. Multiple eigenvalues may be treated by a minor extension of the procedures. The new techniques may be regarded as modifications of the standard Newton-Raphson procedure. Experience indicates that the proposed methods are rapidly convergent and are economical of computational effort.

The numerical procedures developed in this study are applied to buckling and postbuckling of arch members. Numerical results are presented for both in-plane and out-of-plane buckling of an initially planar arch. The results of these various analyses are in good agreement with certain of the previous solutions presented in the literature.

DD FORM 1 NOV 65 1473 (PAGE 1)

S/N 0101-807-6811

Unclassified

Security Classification

A-31408